



## Original article

# Pyrazole-5-carboxamides, novel inhibitors of receptor for advanced glycation end products (RAGE)



Young Taek Han<sup>a,1</sup>, Kyeojin Kim<sup>b,1</sup>, Gyeong-In Choi<sup>b</sup>, Hongchan An<sup>b</sup>, Dohyun Son<sup>c</sup>, Hee Kim<sup>d</sup>, Hee-Jin Ha<sup>d</sup>, Jun-Hyeng Son<sup>b</sup>, Suk-Jae Chung<sup>b</sup>, Hyun-Ju Park<sup>c</sup>, Jeewoo Lee<sup>b</sup>, Young-Ger Suh<sup>b,\*</sup>

<sup>a</sup> College of Pharmacy, Woosuk University, Wanju 565-701, Republic of Korea

<sup>b</sup> College of Pharmacy, Seoul National University, 599 Gwanak-ro, Gwanak-gu, Seoul 151-742, Republic of Korea

<sup>c</sup> School of Pharmacy, Sungkyunkwan University, Suwon 440-746, Republic of Korea

<sup>d</sup> Medifron DBT, Sandanro 349, Danwon-Gu, Ansan-City, Gyeonggi-Do 425-839, Republic of Korea

## ARTICLE INFO

## Article history:

Received 5 November 2013

Received in revised form

18 March 2014

Accepted 25 March 2014

Available online 26 March 2014

## Keywords:

RAGE (receptor for advanced glycation end products)

Alzheimer's disease, RAGE inhibitor

Pyrazole-5-carboxamide

SAR (structure–activity relationship)

## ABSTRACT

In an effort to develop novel inhibitors of receptor for advanced glycation end products (RAGE) for the treatment of Alzheimer's disease, a series of pyrazole-5-carboxamides were designed, synthesized and biologically evaluated. Analyses of the extensive structure–activity relationship (SAR) led us to identify a 4-fluorophenoxy analog (**40**) that exhibited improved in vitro RAGE inhibitory activity and more favorable aqueous solubility than the parent 2-aminopyrimidine, **1**. Surface plasmon resonance (SPR) and molecular docking study strongly supported the RAGE inhibitory activity of pyrazole-5-carboxamides. The brain A $\beta$ -lowering effect of **40** is also described.

© 2014 Elsevier Masson SAS. All rights reserved.

## 1. Introduction

Alzheimer's disease (AD) is the most common cause of dementia in the elderly population. This disease is characterized by the accumulation of amyloid- $\beta$  (A $\beta$ ) plaques and neurofibrillary tangles, which are accompanied by progressive neuronal cell death [1]. According to the prevailing amyloid cascade hypothesis [2], A $\beta$  monomers are generated from amyloid precursor protein (APP), are composed almost entirely of somatic cells, and spontaneously assemble into small aggregates, such as oligomers and fibrils. These soluble A $\beta$  aggregates accumulate in the brain and eventually form insoluble A $\beta$  plaques, a hallmark of AD. Therefore, the accumulation

of soluble A $\beta$  in the brain is a crucial step leading to neuronal toxicity in AD. Promotion of A $\beta$  accumulation in the brain can be caused by the increased production and decreased clearance of A $\beta$ . Increased A $\beta$  production is generally the result of an inherited genetic problem and has only been observed in a relatively small number (<5%) of AD patients. The majority of AD patients does not display increased A $\beta$  production but rather decreased A $\beta$  clearance in the brain as a result of complex causes [3].

As an important part of the A $\beta$  clearance system [4], specific receptors and a carrier-mediated transport system at the blood–brain barrier (BBB) regulate the entry of plasma-derived A $\beta$  into the brain and the clearance of brain-derived A $\beta$ . Low-density lipoprotein receptor-related protein-1 (LRP-1) mediates A $\beta$  efflux from the brain, and RAGE, a multi-ligand receptor on the cell surface, binds soluble A $\beta$  and mediates influx into the brain [5]. RAGE not only is responsible for the transport of soluble A $\beta$  into the brain [6] but also activates nuclear factor- $\kappa$ B (NF- $\kappa$ B) [7], a crucial transcription factor in various inflammatory responses. RAGE is expressed at low concentrations under normal physiological conditions, with the exception of embryonic development [8], but generally becomes up-regulated in the brains of AD patients through a positive feedback loop generated by the NF- $\kappa$ B-responsive element in the RAGE

**Abbreviations:** RAGE, receptor for advanced glycation end products; SAR, structure–activity relationship; SPR, surface plasmon resonance; AD, Alzheimer's disease; APP, amyloid precursor protein; BBB, blood–brain barrier; LRP-1, low-density lipoprotein receptor-related protein-1; NF- $\kappa$ B, nuclear factor- $\kappa$ B; sRAGE, soluble RAGE; HTS, high throughput screening; ELISA, enzyme-linked immunosorbent assay.

\* Corresponding author.

E-mail address: [ygsuh@snu.ac.kr](mailto:ygsuh@snu.ac.kr) (Y.-G. Suh).

<sup>1</sup> These two authors have contributed equally to this work.

gene promoter [9,10]. These mechanisms lead to progressive aggravation of AD due to continuous increases in soluble A $\beta$  influx into the brain and subsequent inflammatory responses. Recently, a number of studies have suggested that the primary pathogenic form of A $\beta$  is not amyloid plaques, but soluble A $\beta$  oligomers [11,12]. Based on these data, inhibition of the RAGE-A $\beta$  interaction may be a promising disease-modifying approach for the treatment of AD [13] by decreasing the toxic levels of soluble A $\beta$  in the brain, thereby reducing subsequent neurotoxic events.

In recent decades, numerous studies have been conducted regarding the therapeutic effects of inhibition of RAGE-A $\beta$  interaction using protein inhibitors, such as RAGE antibodies and soluble RAGE (sRAGE), a truncated soluble extracellular binding domain of RAGE [14,15]. However, reports of small-molecule RAGE inhibitors have been far less common up to date. To the best of our knowledge, only one compound, which was developed by Pfizer (PF-04494700), has entered a clinical trials (phase II) [16,17], and Zlokovic and his colleagues have reported the identification of multi-modal RAGE inhibitors through high throughput screening (HTS) of a chemical library [18]. Recently, we also reported a series of 2-aminopyrimidines as novel RAGE inhibitor [19]. The 2-aminopyrimidines were designed based on the structure of argpyrimidine, a monomeric advanced glycation end product (AGE). We investigated the ability of several amino acid moiety equivalents to modify the structural and electronic properties of argpyrimidine. Consequently, we identified both the robust linker and terminal polar moieties of the active structures. Finally, RAGE inhibitors including 4,6-bis(4-chlorophenyl)pyrimidine (**1**), a representative inhibitor that exhibited significant therapeutic effects in an AD model study, were identified through extensive SAR studies. The previous SAR analysis on the 2-aminopyrimidine analogs implied that the *N,N*-diethylaminoalkoxyphenylamine side chain would be more essential than the aryl-substituted *N*-heterocyclic portion for RAGE inhibitory activity. Based on this observation, we extended our work to explore novel aryl-substituted heterocyclic scaffolds, which may improve both the RAGE inhibitory activities and the physicochemical properties of the inhibitors. Thus, we investigated a series of aryl-substituted heterocyclic systems possessing the essential *N,N*-diethyl phenoxyalkylamine moiety, and identified a novel scaffold of 3-(4-methoxyphenyl)-pyrazole-5-carboxamides (**2**). Herein, we report the identification of novel and advanced RAGE inhibitors of pyrazole-5-carboxamides and the results of the SAR study, which include optimization of the pyrazole scaffold and the aminoalkoxyphenyl side chain (Fig. 1). In addition,

analyses of the direct binding of the identified pyrazole-5-carboxamides to RAGE using SPR studies are described. The binding modes of the pyrazole-5-carboxamides were predicted using a molecular docking study. Finally, studies of the *in vivo* A $\beta$ -lowering effect, including the solubilities of the identified RAGE inhibitors, are presented.

## 2. Results and discussions

### 2.1. Chemistry

Preparation of the *N*-methyl pyrazole-5-carboxylates **7a–e** [20] was achieved according to the sequence of reactions described in Scheme 1. Silyloxyacetophenone (**5b**) [21] and pyridinylacetophenone (**5d**) were synthesized from hydroxyacetophenone (**3**) via TBS protection and an aromatic substitution reaction with 2-bromopyridine, respectively. Biaryl ethers **5c** and **5e** were readily prepared from 4-fluoroacetophenone (**4**) via an aromatic substitution reaction with a corresponding phenol. Claisen condensations of commercially available 4-methoxyacetophenone **5a** and 4-substituted acetophenones **5b–e** with diethyl oxalate and subsequent condensation with hydrazine hydrate yielded the 1*H*-pyrazoles **6a–e**, which were subjected to *N*-methylation, resulting in the formation of the *N*-methyl pyrazole-5-carboxylates **7a–e**.

As shown in Scheme 2, isoxazole **8** and *N*-alkyl pyrazoles **9–10** were readily prepared from the chlorophenoxy pyrazole intermediate **7c**. Isoxazole **8** was synthesized from acetophenone **5c** by successive condensations with diethyl oxalate and with hydroxylamine. *N*-alkylations of *H*-pyrazole **6c** with ethyl halide provided *N*-ethyl pyrazole **9** as a single isomer, whereas *N*-Alkylation of **6c** with the corresponding alkyl halide provided the *N*-propyl pyrazole **10** and the *N*-butyl pyrazole **11** along with the separable regioisomers **10'** (17:1) and **11'** (13:1).

A variety of 3-phenoxy pyrazole-5-carboxylates **13a–j** was prepared using a versatile synthetic procedure, as shown in Scheme 3. Deprotection of silyl ether **7b** yielded phenol **12**, which was subjected to coupling reaction [23] with various boronic acids, resulting in the formation of biaryl ethers **13b–j**. Cyclohexyl ether **13a** was readily synthesized from **12** through a Mitsunobu reaction with cyclohexanol.

To synthesize the carboxamide analogs, anilines **18a–c** were initially prepared as outlined in Scheme 4. Mitsunobu reaction of commercially available 5-fluoro-2-nitrophenol (**14**) with *n*-butanol afforded ether **15**, which was subjected to aromatic substitution to

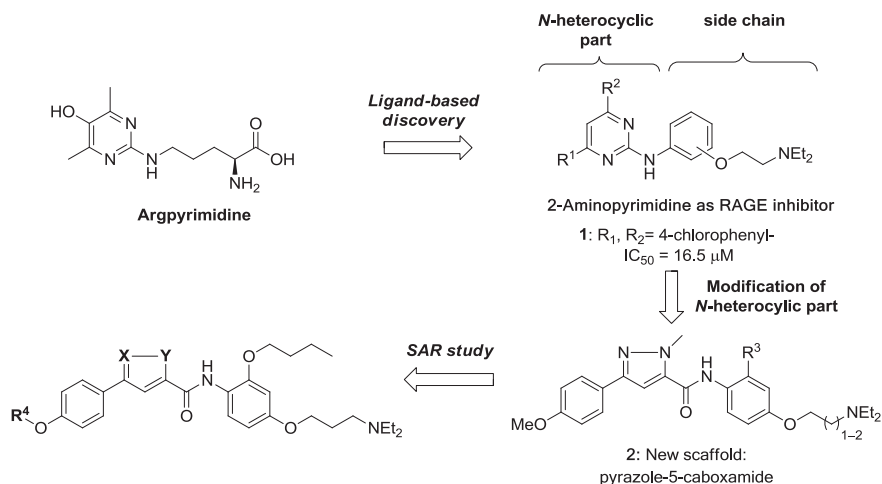
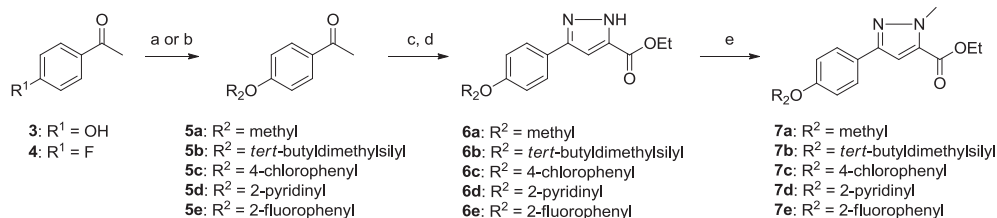
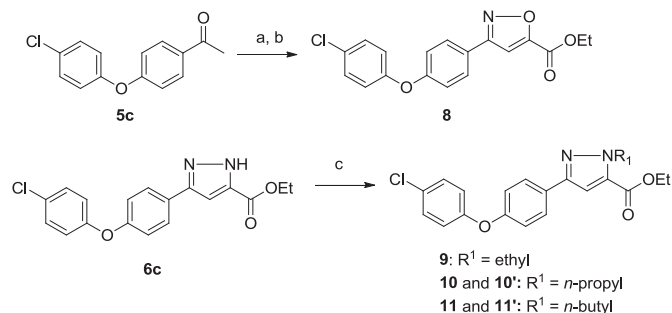


Fig. 1. Overview of previous work and the new strategy for the development of novel RAGE inhibitors of pyrazole-5-carboxamide.



**Scheme 1.** Reagents and conditions: (a) *tert*-butyldimethylsilyl chloride, imidazole, DMF, rt, 95% for **5b**; (b) phenol or 2-bromopyridine, K<sub>2</sub>CO<sub>3</sub>, DMF, 150 °C, 24 h, 79–94% for **5a** and **5c–5d**; (c) TMS<sub>2</sub>NLi, diethyl oxalate, THF, 0 °C → rt, 1 h; (d) NH<sub>2</sub>NH<sub>2</sub>·H<sub>2</sub>O, AcOH, rt, 3 h, 65–88% for 2 steps; (e) MeI, K<sub>2</sub>CO<sub>3</sub>, DMF, rt, 68–95%. The structures of **7a** was confirmed by comparison of the spectral data with those of the corresponding known isomer [22].

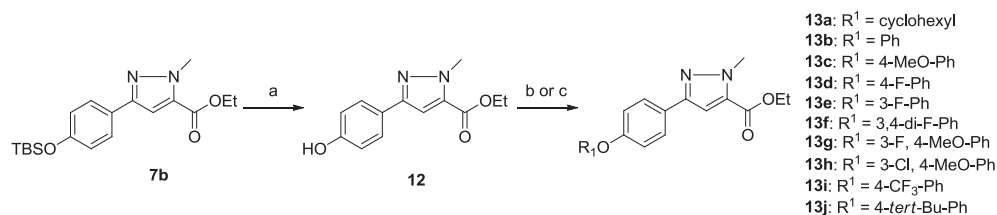


**Scheme 2.** Reagents and conditions: (a) TMS<sub>2</sub>NLi, diethyl oxalate, THF, 0 °C → rt, 1 h; (b) hydroxylamine hydrochloride, EtOH, reflux, 48 h, 74% in 2 steps; (c) RX, K<sub>2</sub>CO<sub>3</sub>, DMF, rt, 90–96%.

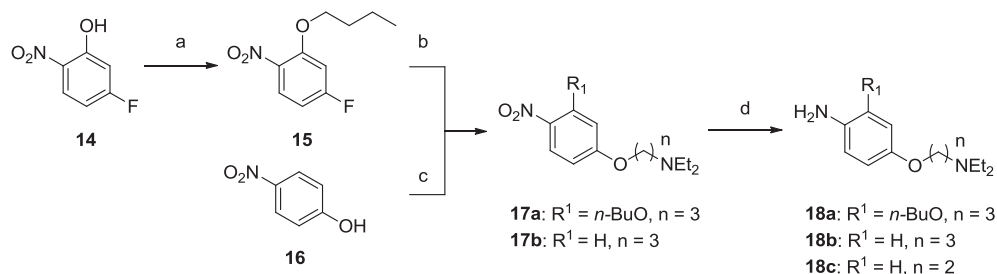
yield nitrophenyl ether **17a**. Nitrophenyl ether **17b** was synthesized from nitrophenol **16** by Mitsunobu reaction. Aminophenyl ethers **18a** and **18b** were synthesized from nitrophenyl ethers **17a** and **17b**, respectively, according to the synthetic procedure used to generate **18c** [19]. Finally, hydrolysis of the ethyl carboxylates (**7a–e**, **8–11** and **13a–13j**) readily provided the corresponding pyrazole-5-carboxylic acids, which were subjected to amidation with anilines **18a–c** to yield the desired carboxamide analogs **19–45** (Scheme 5).

## 2.2. Identification of the pyrazole-5-carboxamide scaffold for novel RAGE inhibitors

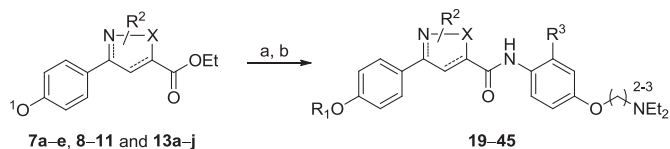
The initial step in the development of novel RAGE inhibitors focused on the identification of a new *N*-heterocyclic scaffold. Using an enzyme-linked immunosorbent assay (ELISA) [19], we initially evaluated a variety of aryl-substituted *N*-heterocyclic systems, such as triazoles, quinazolines, triazines and pyridazines. Disappointingly, we were unable to observe a significant RAGE inhibition using the examined *N*-heterocyclic systems (data not shown). In contrast, as shown in Table 1, a series of 3-(methoxyphenyl)-pyrazole-5-carboxamides (**19–21**), with the exception of *1H*-pyrazole (**22**), consistently exhibited weak RAGE inhibitory activities. To further evaluate the use of pyrazole-5-carboxamide as a novel scaffold for the development of RAGE inhibitors, we synthesized and evaluated a series of 4-chlorophenoxy analogs **23–25**, which were designed based on the structures of the initially identified RAGE inhibitors. As we anticipated [19], the 4-chlorophenoxy analogs (**23–25**) exhibited higher RAGE inhibitory activities than the corresponding methoxy analogs (**19–21**). In particular, butoxy analogs **21** and **25** displayed high inhibitory activities compared to analogs **19** and **23**. Based on these results, we confirmed that a pyrazole-5-carboxamide containing the 2-butoxy-4-(diethylaminopropoxy)aniline moiety could be used as a scaffold for the development of novel RAGE inhibitors.



**Scheme 3.** Reagents and conditions: (a) tetra-*n*-butylammonium fluoride, THF, rt, 92%; (b) cyclohexanol, diisopropylazodicarboxylate, PPh<sub>3</sub>, THF, rt, overnight, 95%; (c) boronic acid, Cu(OAc)<sub>2</sub>, Et<sub>3</sub>N, 4 Å MS, CH<sub>2</sub>Cl<sub>2</sub>, rt, 24 h, 15–73%.



**Scheme 4.** Reagents and conditions: (a) *n*-butanol, diisopropylazodicarboxylate, PPh<sub>3</sub>, THF, rt, 1 h, 96%; (b) 3-diethylamino-1-propanol, 60% NaH in mineral oil, THF, reflux, 24 h, 58%; (c) 3-diethylamino-1-propanol, diisopropylazodicarboxylate, PPh<sub>3</sub>, THF, rt, 1 h, 89%; (d) SnCl<sub>2</sub>·2H<sub>2</sub>O, EtOH, reflux, 3 h, 89% for **18a** and 91% for **18b**.



**Scheme 5.** Reagents and conditions: (a) LiOH·H<sub>2</sub>O, THF/MeOH/H<sub>2</sub>O (5:1:1), rt; (b) oxalyl chloride, DMF, CH<sub>2</sub>Cl<sub>2</sub>, 0 °C → rt, 1 h, then **18a–c**, Et<sub>3</sub>N, THF, rt, 1 h, 37–77%.

### 2.3. SAR study of the pyrazole-5-carboxamide analogs

Based on the promising in vitro activities of the initial pyrazole-5-carboxamide analogs, an SAR study based on the structure of the butoxy analogs (**21** and **25**) was conducted, and the results are summarized in Table 2. First, we investigated the *N*-methyl-pyrazole moiety of chlorophenyl analog **25**. 1*H*-Pyrazole **26** did not display the RAGE inhibitory activity that was displayed by analog **22**, which contains a methoxy-substituent instead of the chloro-substituent contained in **26**. Interestingly, *N*-alkylpyrazoles (**28–31** and **33**) and a bioisosteric isoxazole (**27**) exhibited moderate RAGE inhibitory activities. These results implied that the pyrazole moiety may act as a hydrogen bonding acceptor [24], or may conceal the free hydrogen in the pyrazole moiety, which is crucial for the requisite RAGE inhibition. In particular, we observed noticeable difference in the RAGE inhibitory activities of *N*-butyl pyrazoles **31–33**, while both *N*-propyl pyrazoles **29** and its isomer **30** exhibited good inhibitory activities. *N*-Butyl pyrazole **32** did not

**Table 1**  
In vitro RAGE inhibitory activities of the initial pyrazole-5-carboxamide analogs, **19–25**.

Analog	Structure	Inhibition (%) <sup>a</sup>
<b>19</b>		20.5 ± 1.1
<b>20</b>		20.5 ± 2.6
<b>21</b>		32.4 ± 0.5
<b>22</b>		NA <sup>b</sup>
<b>23</b>		27.0 ± 3.7
<b>24</b>		33.8 ± 0.4
<b>25</b>		49.7 ± 2.6

<sup>a</sup> % inhibition values were determined in duplicate experiments with 20 μM concentrations of the analogs and are expressed as the means ± standard deviation.

<sup>b</sup> Not active.

**Table 2**  
In vitro RAGE inhibitory activities of the pyrazole-5-carboxamides, **26–45**.

Analog	R <sub>1</sub>	R <sub>2</sub>	R <sub>3</sub>	Inhibition (%) <sup>a</sup>	IC <sub>50</sub> (μM) <sup>b</sup>
<b>26</b>				NA <sup>c</sup>	ND <sup>d</sup>
<b>27</b>				32.1 ± 1.1	ND
<b>28</b>				44.7 ± 3.4	ND
<b>29</b>				44.6 ± 6.9	ND
<b>30</b>				45.7 ± 7.2	ND
<b>31</b>				36.0 ± 2.5	ND
<b>32</b>				NA	ND
<b>33</b>				41.4 ± 1.9	ND
<b>34</b>				76.0 ± 2.5	2.5
<b>35</b>				77.0 ± 2.9	5.4
<b>36</b>				52.6 ± 1.6	18.9
<b>37</b>				74.2 ± 1.4	7.8
<b>38</b>				NA	ND
<b>39</b>				83.1 ± 0.5	1.9
<b>40</b>				79.3 ± 0.7	1.9
<b>41</b>				37.0 ± 5.2	ND
<b>42</b>				29.5 ± 5.4	ND

(continued on next page)

Table 2 (continued)

Analog	R <sub>1</sub>	R <sub>2</sub>	R <sub>3</sub>	Inhibition (%) <sup>a</sup>	IC <sub>50</sub> (μM) <sup>b</sup>
43				19.9 ± 2.4	ND
44				36.5 ± 6.1	5.3
45				34.1 ± 0.0	ND

<sup>a</sup> % inhibition values were determined in duplicate experiments using 20 μM concentration of the analogs and are expressed as the means ± standard deviation.

<sup>b</sup> The IC<sub>50</sub> values were determined from a serial dilution test using Sigma Plot (Systat Software Inc., CA).

<sup>c</sup> Not active.

<sup>d</sup> Not determined.

exhibit RAGE inhibition. However, the regioisomer **31** and analog **33**, which do not contain the butoxy-substituent, exhibited moderate to good inhibitory activities. These results support the necessity of the *N*-alkyl substituent of the pyrazole moiety for good activity, although the steric interaction between the *N*-alkyl substituent of the pyrazole moiety and the butoxy-substituent on the aromatic ring may not be tolerable.

Inspired by the significant improvement in RAGE inhibition after incorporating the chlorophenyl moiety as shown in the initial analogs **23–25**, we extended the SAR study to the biaryl moiety of the *N*-methyl pyrazole series. Generally, most of the substituents seemed to increase the inhibitory activity, regardless of the substitution pattern, compared the methyl substituent of analog **21**. Increased activities were observed not only for analog **34**, which possesses a cyclohexyl substituent but also for the aryl-substituted analogs, including the phenyl (**35**), pyridinyl (**36**), and 4-methoxyphenyl (**37**) substituents. It is noteworthy that the introduction of electronegative substituents, including 4-trifluoromethylphenyl (**39**) and 4-fluorophenyl (**40**) groups, significantly increased the inhibitory activities (IC<sub>50</sub> = 1.9 μM) compared to the previously reported 2-aminopyrimidine inhibitor **1** (IC<sub>50</sub> = 16.5 μM). *tert*-Butylphenyl analog **38** did not exhibit inhibitory activity, which implies that sterically bulky substituents are not tolerated. We also investigated the effects of the substituent position and additional substitution on the phenoxy moiety. The RAGE inhibitory activities decreased in the order of *para* (**40**, 79.3%), *meta* (**41**, 37.0%), and *ortho* (**42**, 29.5%) for fluoro-substituted biaryl ether analogs. Generally, additional substitution on the phenoxy moiety (**43–45**) decreased the activities.

#### 2.4. Studies of direct binding of the pyrazole-5-carboxamide analog with RAGE

As described above, we developed a novel series of RAGE-inhibitory pyrazole-5-carboxamides by identifying a new scaffold and conducting an SAR study. In addition, several *N*-methyl pyrazole-5-carboxamides including the most active analogs **39** and **40**, exhibited higher inhibitory activities than the previously reported 4,6-disubstituted 2-aminopyrimidines [19]. We were also interested in determining the binding affinities of the pyrazole-5-carboxamide analogs with RAGE, which may be related to the improved inhibitory activities. Thus, we examined the interaction between a representative analog **40**, which is less hydrophobic than **39**, and RAGE. As shown in Fig. 2, we observed a direct interaction

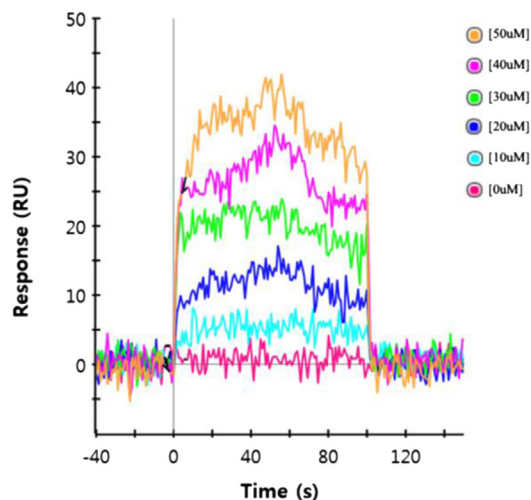
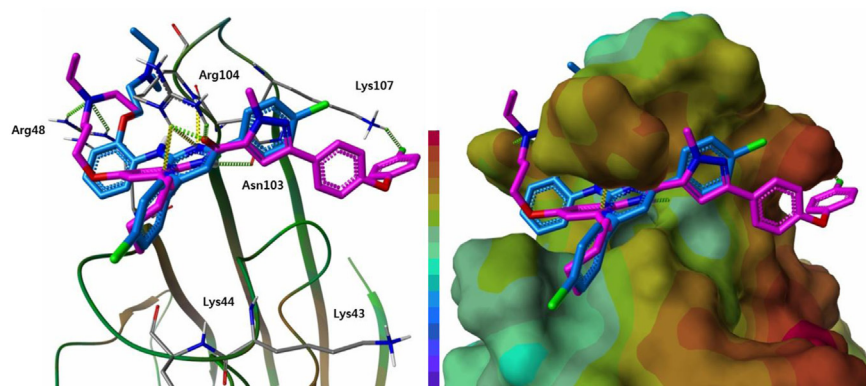


Fig. 2. SPR study of the binding of analog **40** to RAGE. The real-time interaction of **40** with biotinylated RAGE was assessed by measuring the surface plasmon resonance (SPR). RU, resonance units. Typical SPR response curves were measured using a series of concentrations of the tested compounds. The response values were normalized by subtracting the response value of the empty channel. The kinetic and equilibrium constants, listed in the text, were obtained by a global fit, using the Langmuir 1:1 bimolecular kinetic model.

between **40** and RAGE, with a  $K_D$  value of  $4.34 \times 10^{-5}$  M. The binding affinity of pyrazole-5-carboxamide **40** was higher than that of 2-aminopyrimidine **1** ( $K_D = 1.02 \times 10^{-4}$  M) [19,25]. This result shows that the increased potency of **40** is primarily due to its improved RAGE-binding affinity.

To examine the binding mode of **40** in comparison with that of **1**, we performed molecular docking analyses of **1** and **40** using the V-domain of RAGE. In accord with our previous report [19], the active site was defined as the known AGE binding site [25], which is surrounded by positively charged amino acid residues such as Lys43, Lys44, Arg48, and Arg104 (model 1). With the exception of the 4-fluorophenoxy phenyl moiety, the molecular structure of **40** (magenta) is superimposed over the full structure of **1** in the active site of RAGE (Fig. 3). The extended 4-fluorophenoxy phenyl moiety of **40** snugly fits into the electro-positive groove and the 4-fluoro substituent forms a hydrogen bond with the NH<sub>2</sub> in Lys107. Molecular modeling predicted the protonation of NH<sub>2</sub> in Lys107 and a distance of 2.47 Å between NH<sup>+</sup> and F in the 4-fluorophenoxy phenyl moiety. Binding of the phenoxy phenyl moiety in the electro-positive groove may be induced by  $\pi$ -cation (induced dipole moment) interaction, which is one of the key nonbonding interactions for ligand recognition in the receptor binding site [26]. In the structures of various functional proteins complexed with fluorinated compounds, the fluorine atom is located within hydrogen bonding distance from OH or NH of the amino acid residues and can form favorable dipole or hydrogen bond interactions [27–30]. In addition, the NH<sup>+</sup>–F interaction was reported to increase the binding affinity to a much greater extent than the corresponding NH–F interaction [31,32]. The docking model of **40**, compared to that of **1**, revealed a good correlation between the biological activity and binding mode. The additional  $\pi$ -cation interaction and charged hydrogen-bond with Lys107 that were induced by the 4-fluorophenoxy phenyl moiety of **40** may have enhanced the binding affinity and subsequent shielding of the electron-positive A $\beta$ -binding site in RAGE.

The binding site for A $\beta$  is known to be located in a positively charged region, which is widely spread over the V-domain of RAGE. The residues on the positively charged surface of RAGE include: Arg29, Lys37, Lys39, Lys43, Lys44, Arg48, Lys52, Arg98, Arg98,



**Fig. 3.** Left) Overlay of docking poses of **40** (magenta carbon) with **1** (blue carbon) in the AGE-binding site of RAGE (model 1). Hydrogen bonds between **1** and **40** and the receptor are indicated using yellow and green dotted lines, respectively. Key residues of the receptor are displayed as sticks (gray carbon). The green and brown cartoons demonstrate the backbone of RAGE. (Right) The surface of RAGE was rendered based on the electrostatic properties; a color gradient from red to violet is used to color the molecular surface, where red and violet indicate positive and negative electrostatic surface potential, respectively. (For interpretation of the references to colour in this figure legend, the reader is referred to the web version of this article.)

Arg104, Lys107, Lys110, Arg114, and Arg116 [33]. In addition to the binding site used in the docking model shown in Fig. 3, A $\beta$  may possibly bind into the region consisting of Lys37, Lys39, Lys52, Arg98, and Lys110. Therefore, we built another feasible docking model (model 2) for the alternative binding site [Fig. S1 in the Supplementary Content]. Both inhibitors **40** and **1** fit into this binding pocket well, although the calculated binding energy scores ( $-\log K_d$ ) were approximately 3 log units lower [Table S1 in the Supplementary Content] than those obtained using docking model 1 shown in Fig. 3.

### 2.5. Studies of the A $\beta$ -lowering effect and aqueous solubility of pyrazole-5-carboxamides

We performed an acute model study using the representative RAGE inhibitor **40** to confirm the contribution of the RAGE inhibitory activity to the desired down-regulation of A $\beta$  brain entry after preliminary investigation of in vivo exposure [Table S2 in the Supplementary Content] [34]. Pyrazole-5-carboxamides **40** was intraperitoneally injected into wild-type mice prior to human A $\beta$  injection. Inhibition of A $\beta$  brain entry was evaluated by measuring the amount of human A $\beta$  in the brain extracts of the mice [19]. As shown in Table 3, we observed significant brain A $\beta$ -lowering effects without changing the amount of peripheral human A $\beta$ .

Previously, we identified 2-aminopyrimidine **1**, which exhibited significant brain A $\beta$ -lowering effects. Nevertheless, the poor aqueous solubility of **1** has remained a barrier to therapeutic use. Consequently, improved aqueous solubility of the next generation of RAGE inhibitors, including pyrazole-5-carboxamide **40**, is necessary. As anticipated, pyrazole-5-carboxamide **40** exhibited a 4.7-fold increase in solubility [35] compared to **1** (Table 4).

**Table 3**

Brain A $\beta$ -lowering effect of pyrazole-5-carboxamide **40**. The levels of human A $\beta$  in the brain and plasma of mice were measured following tail vein injections of the vehicle or analogs. The concentrations of human A $\beta$  in mice were expressed as the means  $\pm$  standard deviation. Twenty-five milligrams per kilogram of **40** was injected into male ICR mice ( $n = 4$ ).

Human A $\beta$	Control	A $\beta$ only	<b>40</b> + A $\beta$	Reduction (%)
Brain <sup>a</sup>	0.00 $\pm$ 26.37	62.94 $\pm$ 11.96	*39.11 $\pm$ 8.93	37.86
Plasma <sup>b</sup>	0.00 $\pm$ 0.00	676.90 $\pm$ 149.50	704.10 $\pm$ 70.94	-4.01

\* $P < 0.05$ .

<sup>a</sup> pg/mg protein of the brain extracts.

<sup>b</sup> ng/mL of plasma.

### 3. Conclusion

For development of novel RAGE inhibitors for use as potential AD therapeutics, we designed and synthesized a series of pyrazole-5-carboxamides, which were determined to be excellent RAGE inhibitors. We also established the structure–activity relationship of the pyrazole-5-carboxamide inhibitors based on their in vitro RAGE inhibition. In particular, we identified the promising fluoride substituted analogs **39** and **40**, which exhibited higher RAGE inhibitory activity than the parent pyrimidine inhibitor **1**. SPR analysis and a molecular docking study of **40** also supported the hypothesis that the direct binding of pyrazole-5-carboxamide including the representative inhibitor **40**, with RAGE may contribute to the improved RAGE-inhibitory activity. Moreover, analog **40** exhibited significant brain A $\beta$ -lowering effects as well as favorable aqueous solubility.

### 4. Experimental section

Unless otherwise noted, all of the starting materials and reagents were obtained commercially and were used without further purification. Tetrahydrofuran was distilled from sodium benzophenone ketyl. Dichloromethane and acetonitrile were freshly distilled from calcium hydride. All of the solvents that were used for routine product isolation and chromatography were of reagent grade and glass distilled. Reaction flasks were dried at 100 °C prior to use, and air and moisture sensitive reactions were performed under argon. Flash column chromatography was performed using silica gel 60 (230–400 mesh, Merck) with the indicated solvents. Thin-layer chromatography was performed using 0.25 mm silica gel plates (Merck). Mass spectra were obtained using a VG Trio-2 GC–MS instrument, and high resolution mass spectra were obtained using a JEOL JMS-AX 505WA unit. Infrared spectra were recorded on a JASCO FT/IR-4200 spectrometer. <sup>1</sup>H and <sup>13</sup>C spectra were recorded on a JEOL JNM-LA 300, Bruker Analytik ADVANCE

**Table 4**

Kinetic solubility tests for 2-aminopyrimidine (**1**) and pyrazole-5-carboxamide (**40**). Solubilities were determined in triplicate experiments using a DMSO stock solution of the HCl salts of each analog. NEPHELOstar Galaxy (BMG Labtech) was used for nephelometry.

Solubility ( $\mu$ M)	<b>1</b>	<b>40</b>
PBS (pH = 7.4)	16.54 $\pm$ 0.51	80.34 $\pm$ 4.5

digital 400, ADVANCE digital 500 or JEOL ECA-600 spectrometer in deuteriochloroform (CDCl<sub>3</sub>) or deuteriomethanol (CD<sub>3</sub>OD). Chemical shifts are expressed in parts per million (ppm,  $\delta$ ) downfield from tetramethylsilane and are referenced to the deuterated solvent (CHCl<sub>3</sub>). <sup>1</sup>H NMR data are reported in the order: chemical shift, multiplicity (s, singlet; bs, broad singlet; d, doublet; t, triplet; q, quartet; m, multiplet, and/or multiple resonance), numbers of protons, and coupling constants in hertz (Hz). All the final compounds were purified to greater than 95% purity. The purities were determined using a reverse-phase high-performance liquid chromatography (Waters, 254 nm) with an Eclipse Plus C18 (4.6 × 250 mm) and an isocratic flow (MeOH:H<sub>2</sub>O = 9:1) at 1.5 mL/min.

#### 4.1. Synthesis of ethyl carboxylates

##### 4.1.1. 1-(4-(4-Chlorophenoxy)phenyl)ethanone (5c)

To a solution of 4-fluoroacetophenone **4** (2.0 g, 14.48 mmol) and K<sub>2</sub>CO<sub>3</sub> (6.0 g, 43.44 mmol) in dry DMF (20 mL) was added 4-chlorophenol (2.8 g, 21.72 mmol) at ambient temperature. The reaction mixture was stirred for 24 h at 150 °C, cooled to room temperature, and diluted with EtOAc. The organic phase was washed with water and brine, dried over MgSO<sub>4</sub>, and concentrated in vacuo. Purification of the residue via flash column chromatography on silica gel (EtOAc/*n*-hexane/CH<sub>2</sub>Cl<sub>2</sub> = 1:30:0.5) afforded 3.35 g (94%) of acetophenone **5c** as white solid with a melting point of 63–66 °C: <sup>1</sup>H NMR (300 MHz, CDCl<sub>3</sub>)  $\delta$  7.93 (d, 2H, *J* = 8.8 Hz), 7.33 (d, 2H, *J* = 8.6 Hz), 7.01–6.96 (m, 4H), 2.56 (s, 3H); LRMS (FAB) *m/z* 247 (M + H<sup>+</sup>).

##### 4.1.2. 1-(4-(Pyridin-2-yloxy)phenyl)ethanone (5d)

To a solution of 4-hydroxyacetophenone **3** (500 mg, 3.67 mmol) and K<sub>2</sub>CO<sub>3</sub> (1.5 g, 11.01 mmol) in dry DMF (10 mL) was added 2-bromopyridine (0.54 mL, 3.67 mmol) at ambient temperature. The reaction mixture was stirred for 24 h at 150 °C, cooled to room temperature, and diluted with EtOAc. The organic phase was washed with water and brine, dried over MgSO<sub>4</sub>, and concentrated in vacuo. Purification of the residue via flash column chromatography on silica gel (EtOAc/*n*-hexane = 1:5) afforded 618 mg (79%) of acetophenone **5d** as white solid with a melting point of 104–106 °C: <sup>1</sup>H NMR (300 MHz, CDCl<sub>3</sub>)  $\delta$  8.20 (dd, 1H, *J* = 1.5, 4.9 Hz), 7.99 (d, 2H, *J* = 8.8 Hz), 7.76–7.70 (m, 1H), 7.18 (d, 2H, *J* = 8.8 Hz), 7.07–7.03 (m, 1H), 6.98 (d, 1H, *J* = 8.3 Hz), 2.58 (s, 3H); LRMS (FAB) *m/z* 214 (M + H<sup>+</sup>).

##### 4.1.3. 1-(4-(2-Fluorophenoxy)phenyl)ethanone (5e)

Acetophenone **5e** was prepared from **4** (0.2 mL, 1.65 mmol) by the procedure for **5c**, using 2-fluorophenol (0.22 mL, 2.47 mmol) instead of 4-chlorophenol. Purification of the residue via flash column chromatography on silica gel (EtOAc/*n*-hexane/CH<sub>2</sub>Cl<sub>2</sub> = 1:30:0.5) afforded 353 mg (93%) of acetophenone **5e** as white solid with a melting point of 52–53 °C: <sup>1</sup>H NMR (300 MHz, CDCl<sub>3</sub>)  $\delta$  7.92 (d, 2H, *J* = 9.0 Hz), 7.22–7.13 (m, 4H), 6.96 (d, 2H, *J* = 8.6 Hz), 2.55 (s, 3H); LRMS (FAB) *m/z* 231 (M + H<sup>+</sup>).

##### 4.1.4. Ethyl 3-(4-methoxyphenyl)-1H-pyrazole-5-carboxylate (6a)

To a solution of 4-methoxyacetophenone **5a** (1.0 g, 6.66 mmol) in THF (50 mL) was added 1 M LHMDS in THF solution (7.2 mL, 7.20 mmol) at 0 °C. The reaction mixture was stirred for 1 h at the same temperature and diethyl oxalate (1.14 mL, 7.9 mmol) was added. The mixture was stirred for 1 h at ambient temperature, concentrated in vacuo, and diluted with EtOAc. The organic phase was washed with water and brine, dried over MgSO<sub>4</sub>, and concentrated in vacuo. The residue was dissolved in AcOH (7 mL), and hydrazine hydrate (0.41 mL, 13.32 mmol) was added at ambient

temperature. The reaction mixture was stirred for 3 h at the same temperature and H<sub>2</sub>O was slowly added until no more solid precipitated. The solid was collected by filtration and washed with H<sub>2</sub>O and *n*-hexane. Purification of the solid via flash column chromatography on silica gel (EtOAc/*n*-hexane/CH<sub>2</sub>Cl<sub>2</sub> = 1:3:0.5) afforded 1.4 g (84%) of 1H-pyrazole **6a** as white solid with a melting point of 160–161 °C: FT-IR (thin film, neat)  $\nu_{\max}$  3138, 2982, 1726, 1423, 1253, 1029 cm<sup>-1</sup>; <sup>1</sup>H NMR (300 MHz, CDCl<sub>3</sub>)  $\delta$  7.64 (d, 2H, *J* = 9.0 Hz), 7.02 (s, 1H), 6.94 (d, 2H, *J* = 8.2 Hz), 4.39 (q, 2H, *J* = 7.1 Hz), 3.83 (s, 3H), 1.34 (t, 3H, *J* = 7.1 Hz); LRMS (FAB) *m/z* 247 (M + H<sup>+</sup>).

##### 4.1.5. Ethyl 3-(4-((tert-butyl)dimethylsilyloxy)phenyl)-1H-pyrazole-5-carboxylate (6b)

1H-Pyrazole **6b** was prepared by the procedure for **6a**, using **5b** (700 mg, 2.80 mmol) instead of 4-methoxyacetophenone **5a**. Purification of the residue via flash column chromatography on silica gel (EtOAc/*n*-hexane = 1:4) afforded 750 mg (77%) of 1H-pyrazole **6b** as white solid with a melting point of 140–143 °C: FT-IR (thin film, neat)  $\nu_{\max}$  3100, 2930, 2858, 1730, 1471, 1232, 925 cm<sup>-1</sup>; <sup>1</sup>H NMR (300 MHz, CD<sub>3</sub>OD)  $\delta$  7.58 (d, 2H, *J* = 8.8 Hz), 7.01 (s, 1H), 6.88 (d, 2H, *J* = 8.6 Hz), 4.39 (q, 2H, *J* = 7.1 Hz), 1.40 (t, 3H, *J* = 7.1 Hz); LRMS (FAB) *m/z* 347 (M + H<sup>+</sup>).

##### 4.1.6. Ethyl 3-(4-(4-chlorophenoxy)phenyl)-1H-pyrazole-5-carboxylate (6c)

1H-Pyrazole **6c** was prepared by the procedure for **6a**, using **5c** (1.00 g, 4.05 mmol) instead of 4-methoxyacetophenone **5a**. Purification of the residue via crystallization (Et<sub>2</sub>O/*n*-hexane = 1:5) afforded 1.23 g (83%) of 1H-pyrazole **6c** as white solid with a melting point of 182–185 °C: <sup>1</sup>H NMR (300 MHz, CDCl<sub>3</sub>)  $\delta$  7.72 (d, 2H, *J* = 8.4 Hz), 7.29 (d, 2H, *J* = 8.8 Hz), 7.06–7.02 (m, 3H), 6.96 (d, 2H, *J* = 8.8 Hz), 4.40 (q, 2H, *J* = 7.1 Hz), 1.40 (t, 3H, *J* = 7.1 Hz); LRMS (FAB) *m/z* 343 (M + H<sup>+</sup>).

##### 4.1.7. Ethyl 3-(4-(pyridin-2-yloxy)phenyl)-1H-pyrazole-5-carboxylate (6d)

1H-Pyrazole **6d** was prepared by the procedure for **6a**, using **5d** (200 mg, 0.94 mmol) instead of 4-methoxyacetophenone **5a**. Purification of the residue via flash column chromatography on silica gel (EtOAc/*n*-hexane = 1:2) afforded 190 mg (65%) of 1H-pyrazole **6d** as white solid with a melting point of 169–172 °C: <sup>1</sup>H NMR (300 MHz, CDCl<sub>3</sub>)  $\delta$  8.19 (dd, 1H, *J* = 2.0, 4.9 Hz), 7.77–7.67 (m, 3H), 7.19 (d, 2H, *J* = 8.6 Hz), 7.07 (s, 1H), 7.03–6.98 (m, 1H), 6.94 (d, 1H, *J* = 8.3 Hz), 4.40 (q, 2H, *J* = 7.1 Hz), 1.40 (t, 3H, *J* = 7.0 Hz); LRMS (FAB) *m/z* 310 (M + H<sup>+</sup>).

##### 4.1.8. Ethyl 3-(4-(2-fluorophenoxy)phenyl)-1H-pyrazole-5-carboxylate (6e)

1H-Pyrazole **6e** was prepared by the procedure for **6a**, using **5e** (130 mg, 0.56 mmol) instead of 4-methoxyacetophenone **5a**. Purification of the residue via flash column chromatography on silica gel (EtOAc/*n*-hexane = 1:5) afforded 161 mg (88%) of 1H-pyrazole **6e** as white solid with a melting point of 131–135 °C: <sup>1</sup>H NMR (300 MHz, CDCl<sub>3</sub>)  $\delta$  7.70 (d, 2H, *J* = 8.6 Hz), 7.21–7.08 (m, 4H), 7.04–6.99 (m, 3H), 4.39 (q, 2H, *J* = 7.0 Hz), 1.39 (t, 3H, *J* = 7.1 Hz); LRMS (FAB) *m/z* 327 (M + H<sup>+</sup>).

##### 4.1.9. Ethyl 3-(4-methoxyphenyl)-1-methyl-1H-pyrazole-5-carboxylate (7a)

To a solution of 1H-pyrazole **6a** (455 mg, 1.85 mmol) and K<sub>2</sub>CO<sub>3</sub> (384 mg, 2.78 mmol) in dry DMF (5 mL) was added iodometane (0.17 mL, 2.78 mmol) at ambient temperature. The reaction mixture was stirred overnight at the same temperature and diluted with EtOAc. The organic phase was washed with water and brine, dried

over MgSO<sub>4</sub>, and concentrated in vacuo. Purification of the residue via flash column chromatography on silica gel (EtOAc/*n*-hexane = 1:7) afforded 448 mg (93%) of 1-methylpyrazole **7a** as white solid with a melting point of 68–70 °C: <sup>1</sup>H NMR (300 MHz, CDCl<sub>3</sub>) δ 7.67 (d, 2H, *J* = 8.8 Hz), 7.01 (s, 1H), 6.90 (d, 2H, *J* = 8.8 Hz), 4.35 (q, 2H, *J* = 7.1 Hz), 4.20 (s, 3H), 3.91 (s, 3H), 1.39 (t, 3H, *J* = 7.1 Hz); LRMS (FAB) *m/z* 261 (M + H<sup>+</sup>).

#### 4.1.10. Ethyl 3-(4-((*tert*-butyldimethylsilyloxy)phenyl)-1-methyl-1H-pyrazole-5-carboxylate (**7b**)

1-Methylpyrazole **7b** was prepared by the procedure for **7a**, using **6b** (103 mg, 0.30 mmol) instead of **6a**. Purification of the residue via flash column chromatography on silica gel (EtOAc/*n*-hexane = 1:7) afforded 81 mg (76%) of 1-methylpyrazole **7b** as a colorless oil: <sup>1</sup>H NMR (300 MHz, CDCl<sub>3</sub>) δ 7.64 (d, 2H, *J* = 8.4 Hz), 7.04 (s, 1H), 6.86 (d, 2H, *J* = 8.4 Hz), 4.36 (q, 2H, *J* = 7.1 Hz), 4.20 (s, 3H), 1.40 (t, 3H, *J* = 7.1 Hz), 0.98 (s, 9H), 0.20 (s, 6H); LRMS (FAB) *m/z* 361 (M + H<sup>+</sup>).

#### 4.1.11. Ethyl 3-(4-(4-chlorophenoxy)phenyl)-1-methyl-1H-pyrazole-5-carboxylate (**7c**)

1-Methylpyrazole **7c** was prepared by the procedure for **7a**, using **6c** (100 mg, 0.29 mmol) instead of **6a**. Purification of the residue via flash column chromatography on silica gel (EtOAc/*n*-hexane = 1:10) afforded 70 mg (68%) of 1-methylpyrazole **7c** as white solid with a melting point of 80–82 °C: <sup>1</sup>H NMR (300 MHz, CDCl<sub>3</sub>) δ 7.94 (d, 2H, *J* = 8.3 Hz), 7.50–7.44 (m, 3H), 7.23–7.14 (m, 4H), 4.55 (q, 2H, *J* = 7.0 Hz), 4.40 (s, 3H), 1.59 (t, 3H, *J* = 7.0 Hz); LRMS (FAB) *m/z* 357 (M + H<sup>+</sup>).

#### 4.1.12. Ethyl 1-methyl-3-(4-(pyridin-2-yloxy)phenyl)-1H-pyrazole-5-carboxylate (**7d**)

1-Methylpyrazole **7d** was prepared by the procedure for **7a**, using **6d** (170 mg, 0.55 mmol) instead of **6a**. Purification of the residue via flash column chromatography on silica gel (EtOAc/*n*-hexane = 1:4) afforded 177 mg (95%) of 1-methylpyrazole **7d** as white solid with a melting point of 82–86 °C: FT-IR (thin film, neat)  $\nu_{\max}$  2983, 1721, 1468, 1428, 1261 cm<sup>-1</sup>; <sup>1</sup>H NMR (300 MHz, CDCl<sub>3</sub>) δ 8.19 (dd, 1H, *J* = 2.0, 5.0 Hz), 7.80 (d, 2H, *J* = 8.6 Hz), 7.71–7.65 (m, 1H), 7.16 (d, 2H, *J* = 8.6 Hz), 7.07 (s, 1H), 7.01–6.97 (m, 1H), 6.91 (d, 1H, *J* = 8.2 Hz), 4.35 (q, 2H, *J* = 7.1 Hz), 4.20 (s, 3H), 1.39 (t, 3H, *J* = 7.0 Hz); LRMS (FAB) *m/z* 324 (M + H<sup>+</sup>).

#### 4.1.13. Ethyl 3-(4-(2-fluorophenoxy)phenyl)-1-methyl-1H-pyrazole-5-carboxylate (**7e**)

1-Methylpyrazole **7e** was prepared by the procedure for **7a**, using **6e** (160 mg, 0.49 mmol) instead of **6a**. Purification of the residue via flash column chromatography on silica gel (EtOAc/*n*-hexane = 1:10) afforded 132 mg (79%) of 1-methylpyrazole **7e** as a colorless oil: <sup>1</sup>H NMR (300 MHz, CDCl<sub>3</sub>) δ 7.72 (d, 2H, *J* = 8.8 Hz), 7.20–7.07 (m, 4H), 7.04 (s, 1H), 6.99 (d, 2H, *J* = 8.6 Hz), 4.35 (q, 2H, *J* = 7.1 Hz), 4.19 (s, 3H), 1.38 (t, 3H, *J* = 7.1 Hz); LRMS (FAB) *m/z* 341 (M + H<sup>+</sup>).

#### 4.1.14. Ethyl 3-(4-(4-chlorophenoxy)phenyl)isoxazole-5-carboxylate (**8**)

To a solution of **5c** (212 mg, 0.86 mmol) in THF (10 mL) was added 1 M LHMDS in THF solution (0.95 mL, 0.95 mmol) at 0 °C. The reaction mixture was stirred for 1 h at the same temperature and diethyl oxalate (0.15 mL, 1.12 mmol) was added. The reaction mixture was stirred for 1 h at ambient temperature, concentrated in vacuo, and diluted with EtOAc. The organic phase was washed with water and brine, dried over MgSO<sub>4</sub>, and concentrated in vacuo. The residue was dissolved in EtOH (7 mL) and hydroxylamine hydrochloride (60 mg, 0.86 mmol) was added at ambient temperature.

The mixture was refluxed for 48 h and H<sub>2</sub>O was slowly added until no more solid precipitated. The resulting solid was collected by filtration. Purification of the solid via flash column chromatography on silica gel (EtOAc/*n*-hexane/CH<sub>2</sub>Cl<sub>2</sub> = 1:20:1) afforded 218 mg (74%) of isoxazole **8** as white solid with a melting point of 98–100 °C: FT-IR (thin film, neat)  $\nu_{\max}$  3133, 1731, 1485, 1256, 833 cm<sup>-1</sup>; <sup>1</sup>H NMR (300 MHz, CDCl<sub>3</sub>) δ 7.75 (d, 2H, *J* = 9.0 Hz), 7.33 (d, 2H, *J* = 9.0 Hz), 7.06–6.96 (m, 4H), 6.84 (s, 1H), 4.45 (q, 2H, *J* = 7.1 Hz), 1.42 (t, 3H, *J* = 7.1 Hz); LRMS (FAB) *m/z* 344 (M + H<sup>+</sup>).

#### 4.1.15. Ethyl 3-(4-(4-chlorophenoxy)phenyl)-1-ethyl-1H-pyrazole-5-carboxylate (**9**)

1-Ethyl pyrazole **9** was prepared from 1H-pyrazole **6c** (210 mg, 0.61 mmol) by the procedure for **7c**, using iodoethane instead of iodomethane. Purification of the residue via flash column chromatography on silica gel (EtOAc/*n*-hexane = 1:9) afforded 203 mg (90%) of 1-ethyl pyrazole **9** as white solid with a melting point of 86–88 °C: <sup>1</sup>H NMR (300 MHz, CDCl<sub>3</sub>) δ 7.75 (d, 2H, *J* = 8.8 Hz), 7.27 (d, 2H, *J* = 9.2 Hz), 7.05 (s, 1H), 7.01 (d, 2H, *J* = 8.8 Hz), 6.94 (d, 2H, *J* = 9.0 Hz), 4.62 (q, 2H, *J* = 7.1 Hz), 4.35 (q, 2H, *J* = 7.1 Hz), 1.46 (t, 3H, *J* = 7.2 Hz), 1.39 (t, 3H, *J* = 7.1 Hz); LRMS (FAB) *m/z* 371 (M + H<sup>+</sup>).

#### 4.1.16. Ethyl 3-(4-(4-chlorophenoxy)phenyl)-1-propyl-1H-pyrazole-5-carboxylate (**10**) and ethyl 5-(4-(4-chlorophenoxy)phenyl)-1-propyl-1H-pyrazole-3-carboxylate (**10'**)

1-Propyl pyrazole **10** and **10'** were prepared from 1H-pyrazole **6a** (180 mg, 0.53 mmol) by the procedure for **7c**, using 1-iodopropane instead of iodomethane. Purification of the residue via flash column chromatography on silica gel (EtOAc/*n*-hexane = 1:9) afforded 186 mg (91%) of 1-propylpyrazole **10** and 11 mg (5%) of the regioisomer **10'** as a colorless oil: **10**: <sup>1</sup>H NMR (300 MHz, CDCl<sub>3</sub>) δ 7.75 (d, 2H, *J* = 8.4 Hz), 7.27 (d, 2H, *J* = 8.6 Hz), 7.05 (s, 1H), 7.01 (d, 2H, *J* = 8.6 Hz), 6.94 (d, 2H, *J* = 8.6 Hz), 4.53 (t, 2H, *J* = 7.3 Hz), 4.35 (q, 2H, *J* = 7.1 Hz), 1.92–1.85 (m, 2H), 1.39 (t, 3H, *J* = 7.1 Hz), 0.93 (t, 3H, *J* = 7.4 Hz); <sup>13</sup>C NMR (CDCl<sub>3</sub>, 100 MHz) δ 159.5, 156.5, 155.8, 148.9, 133.1, 129.6, 129.6, 128.4, 128.1, 127.0, 127.0, 119.9, 119.9, 119.0, 119.0, 107.6, 60.9, 53.3, 24.0, 14.1, 10.9; LRMS (FAB) *m/z* 385 (M + H<sup>+</sup>). **10'**: <sup>1</sup>H NMR (300 MHz, CDCl<sub>3</sub>) δ 7.34–7.30 (m, 4H), 7.04 (d, 2H, *J* = 8.6 Hz), 6.99 (d, 2H, *J* = 8.8 Hz), 6.76 (s, 1H), 4.40 (q, 2H, *J* = 7.1 Hz), 4.11 (t, 2H, *J* = 7.5 Hz), 1.89–1.76 (m, 2H), 1.38 (t, 3H, *J* = 7.1 Hz), 0.80 (t, 3H, *J* = 7.4 Hz); <sup>13</sup>C NMR (CDCl<sub>3</sub>, 75 MHz) δ 160.5, 157.9, 154.8, 144.1, 142.7, 130.6, 130.6, 130.0, 130.0, 129.2, 124.9, 120.8, 120.8, 118.4, 118.4, 108.9, 60.9, 51.8, 23.8, 14.4, 10.9; LRMS (FAB) *m/z* 385 (M + H<sup>+</sup>).

#### 4.1.17. Ethyl 1-butyl-3-(4-(4-chlorophenoxy)phenyl)-1H-pyrazole-5-carboxylate (**11**) and ethyl 1-butyl-5-(4-(4-chlorophenoxy)phenyl)-1H-pyrazole-3-carboxylate (**11'**)

1-Butylpyrazole **11** and **11'** were prepared from 1H-pyrazole **6c** (100 mg, 0.29 mmol) by the procedure for **7c**, using 1-iodobutane instead of iodomethane. Purification of the residue via flash column chromatography on silica gel (EtOAc/*n*-hexane = 1:9) afforded 102 mg (88%) of 1-butylpyrazole **11** and 8 mg (6%) of the regioisomer **11'** as a colorless oil: **11**: <sup>1</sup>H NMR (300 MHz, CDCl<sub>3</sub>) δ 7.77 (d, 2H, *J* = 8.4 Hz), 7.29 (d, 2H, *J* = 8.8 Hz), 7.07 (s, 1H), 7.02 (d, 2H, *J* = 8.4 Hz), 6.96 (d, 2H, *J* = 8.6 Hz), 4.58 (t, 2H, *J* = 7.4 Hz), 4.36 (q, 2H, *J* = 7.1 Hz), 1.84 (q, 2H, *J* = 7.5 Hz), 1.42–1.35 (m, 4H), 0.95 (t, 3H, *J* = 7.3 Hz); <sup>13</sup>C NMR (CDCl<sub>3</sub>, 75 MHz) δ 159.5, 156.5, 155.7, 148.9, 133.0, 129.6, 129.6, 128.4, 128.1, 127.0, 127.0, 119.8, 119.8, 119.0, 119.0, 107.5, 60.8, 51.6, 32.7, 19.7, 14.1, 13.6; LRMS (FAB) *m/z* 399 (M + H<sup>+</sup>). **11'**: <sup>1</sup>H NMR (300 MHz, CDCl<sub>3</sub>) δ 7.36–7.32 (m, 4H), 7.07–6.99 (m, 4H), 6.78 (s, 1H), 4.42 (q, 2H, *J* = 7.1 Hz), 4.16 (t, 2H, *J* = 7.6 Hz), 1.85–1.75 (m, 2H), 1.43–1.38 (m, 4H), 0.83 (m, 3H, *J* = 7.3 Hz); <sup>13</sup>C NMR (CDCl<sub>3</sub>, 75 MHz) δ 162.5, 157.8, 154.8, 144.0, 142.7, 130.5, 130.5,

129.9, 129.9, 129.1, 124.9, 120.7, 120.7, 118.5, 118.5, 108.8, 60.9, 50.1, 32.4, 19.7, 14.4, 13.5; LRMS (FAB)  $m/z$  399 ( $M + H^+$ ).

#### 4.1.18. Ethyl 3-(4-hydroxyphenyl)-1-methyl-1H-pyrazole-5-carboxylate (**12**)

To a solution of **7b** (74 mg, 0.21 mmol) in THF (2 mL) was added 1 M tetra-*n*-butylammonium fluoride in THF (0.25 mL) at ambient temperature. The reaction mixture was stirred until no starting material was observed by TLC, quenched with H<sub>2</sub>O, and diluted with EtOAc. The organic phase was washed with water and brine, dried over MgSO<sub>4</sub>, and concentrated in vacuo. Crystallization of the residue from Et<sub>2</sub>O (3 mL) afforded 47 mg (92%) of phenol **12** as white solid with a melting point of 188–191 °C: FT-IR (thin film, neat)  $\nu_{\max}$  3136, 1728, 1439, 1257, 1121 cm<sup>-1</sup>; <sup>1</sup>H NMR (300 MHz, CDCl<sub>3</sub>)  $\delta$  7.64 (d, 2H,  $J = 8.4$  Hz), 7.02 (s, 1H), 6.86 (d, 2H,  $J = 8.4$  Hz), 5.37 (bs, 1H), 4.34 (q, 2H,  $J = 7.1$  Hz), 4.18 (s, 3H), 1.38 (t, 3H,  $J = 7.1$  Hz); LRMS (FAB)  $m/z$  247 ( $M + H^+$ ).

#### 4.1.19. Ethyl 3-(4-(cyclohexyloxy)phenyl)-1-methyl-1H-pyrazole-5-carboxylate (**13a**)

To a solution of phenol **12** (20 mg, 0.08 mmol) and triphenylphosphine (28 mg, 0.11 mmol) in THF (2 mL) was added cyclohexanol (11 mg, 0.11 mmol) and diisopropylazodicarboxylate (22  $\mu$ L, 0.11 mmol). The reaction mixture was stirred overnight at ambient temperature, quenched with H<sub>2</sub>O, and diluted with EtOAc. The organic layer was washed with water and brine, dried over MgSO<sub>4</sub> and concentrated in vacuo. Purification of the residue via flash column chromatography on silica gel (EtOAc/*n*-hexane = 1:10) afforded 25 mg (95%) of **13a** as a colorless oil: <sup>1</sup>H NMR (300 MHz, CDCl<sub>3</sub>)  $\delta$  7.68–7.65 (m, 2H), 7.01 (s, 1H), 6.92–6.88 (m, 2H), 4.38–4.23 (m, 3H), 4.19 (s, 3H), 2.02–2.00 (m, 2H), 1.79–1.79 (m, 2H), 1.55–1.32 (m, 9H); LRMS (FAB)  $m/z$  329 ( $M + H^+$ ).

#### 4.1.20. Ethyl 1-methyl-3-(4-phenoxyphenyl)-1H-pyrazole-5-carboxylate (**13b**)

To a solution of phenol **12** (26 mg, 0.11 mmol), phenylboronic acid (20 mg, 0.16 mmol), and copper acetate (23 mg, 0.13 mmol) in the presence of 4 Å molecular sieves in CH<sub>2</sub>Cl<sub>2</sub> (5 mL) was added triethylamine (0.08 mL, 0.55 mmol). The reaction mixture was vigorously stirred for 24 h at ambient temperature and filtered through a Celite pad. The filtrate was concentrated in vacuo and diluted with EtOAc. The organic phase was washed with sat. NH<sub>4</sub>Cl and brine, dried over MgSO<sub>4</sub> and concentrated in vacuo. Purification of the residue via flash column chromatography on silica gel (EtOAc/*n*-hexane = 1:10) afforded 18 mg (53%) of phenyl ether **13b** as white solid with a melting point of 78–81 °C: <sup>1</sup>H NMR (300 MHz, CDCl<sub>3</sub>)  $\delta$  7.74 (d, 2H,  $J = 8.6$  Hz), 7.33 (t, 2H,  $J = 7.9$  Hz), 7.12–7.01 (m, 6H), 4.35 (q, 2H,  $J = 7.1$  Hz), 4.20 (s, 3H), 1.39 (t, 3H,  $J = 7.1$  Hz); LRMS (FAB)  $m/z$  323 ( $M + H^+$ ).

#### 4.1.21. Ethyl 3-(4-(4-methoxyphenoxy)phenyl)-1-methyl-1H-pyrazole-5-carboxylate (**13c**)

Phenylether **13c** was prepared from phenol **12** (30 mg, 0.12 mmol) by the procedure for **13b**, using 4-methoxyphenylboronic acid instead of phenylboronic acid. Purification of the residue via flash column chromatography on silica gel (EtOAc/*n*-hexane = 1:5) afforded 17 mg (40%) of phenyl ether **13c** as a colorless oil: <sup>1</sup>H NMR (300 MHz, CDCl<sub>3</sub>)  $\delta$  7.70 (d, 2H,  $J = 8.4$  Hz), 7.04 (s, 1H), 7.00–6.86 (m, 6H), 4.34 (q, 2H,  $J = 7.1$  Hz), 4.19 (s, 3H), 3.79 (s, 3H), 1.38 (t, 3H,  $J = 7.1$  Hz); LRMS (FAB)  $m/z$  353 ( $M + H^+$ ).

#### 4.1.22. Ethyl 3-(4-(4-fluorophenoxy)phenyl)-1-methyl-1H-pyrazole-5-carboxylate (**13d**)

Phenyl ether **13d** was prepared from phenol **12** (30 mg, 0.12 mmol) by the procedure for **13b**, using 4-fluorophenylboronic

acid instead of phenylboronic acid. Purification of the residue via flash column chromatography on silica gel (EtOAc/*n*-hexane = 1:10) afforded 30 mg (73%) of phenyl ether **13d** as white solid with a melting point of 58–61 °C: <sup>1</sup>H NMR (300 MHz, CDCl<sub>3</sub>)  $\delta$  7.72 (d, 2H,  $J = 9.0$  Hz), 7.05–6.96 (m, 7H), 4.35 (q, 2H,  $J = 7.1$  Hz), 4.20 (s, 3H), 1.39 (t, 3H,  $J = 7.1$  Hz); LRMS (FAB)  $m/z$  341 ( $M + H^+$ ).

#### 4.1.23. Ethyl 3-(4-(3-fluorophenoxy)phenyl)-1-methyl-1H-pyrazole-5-carboxylate (**13e**)

Phenyl ether **13e** was prepared from phenol **12** (30 mg, 0.12 mmol) by the procedure for **13b**, using 3-fluorophenylboronic acid instead of phenylboronic acid. Purification of the residue via flash column chromatography on silica gel (EtOAc/*n*-hexane = 1:10) afforded 24 mg (59%) of phenyl ether **13e** as a colorless oil: <sup>1</sup>H NMR (300 MHz, CDCl<sub>3</sub>)  $\delta$  7.76 (d, 2H,  $J = 8.8$  Hz), 7.29–7.22 (m, 1H), 7.07–7.04 (m, 3H), 6.81–6.75 (m, 2H), 6.71 (td, 1H,  $J = 2.3, 10.1$  Hz), 4.36 (q, 2H,  $J = 7.1$  Hz), 4.20 (s, 3H), 1.39 (t, 3H,  $J = 7.0$  Hz); LRMS (FAB)  $m/z$  341 ( $M + H^+$ ).

#### 4.1.24. Ethyl 3-(4-(3,4-difluorophenoxy)phenyl)-1-methyl-1H-pyrazole-5-carboxylate (**13f**)

Phenyl ether **13f** was prepared from phenol **12** (50 mg, 0.20 mmol) by the procedure for **13b**, using 3,4-difluorophenylboronic acid instead of phenylboronic acid. Purification of the residue via flash column chromatography on silica gel (EtOAc/*n*-hexane = 1:9) afforded 16 mg (22%) of phenyl ether **13f** as a colorless oil: <sup>1</sup>H NMR (300 MHz, CDCl<sub>3</sub>)  $\delta$  7.76 (d, 2H,  $J = 8.8$  Hz), 7.15–7.06 (m, 2H), 7.01 (d, 2H,  $J = 8.8$  Hz), 6.87–6.80 (m, 1H), 6.75–6.74 (m, 1H), 4.35 (q, 2H,  $J = 7.1$  Hz), 4.20 (s, 3H), 1.39 (t, 3H,  $J = 7.1$  Hz); LRMS (FAB)  $m/z$  359 ( $M + H^+$ ).

#### 4.1.25. Ethyl 3-(4-(3-fluoro-4-methoxyphenoxy)phenyl)-1-methyl-1H-pyrazole-5-carboxylate (**13g**)

Phenyl ether **13g** was prepared from phenol **12** (30 mg, 0.12 mmol) by the procedure for **13b**, using 3-fluoro-4-methoxyphenylboronic acid instead of phenylboronic acid. Purification of the residue via flash column chromatography on silica gel (EtOAc/*n*-hexane = 1:6) afforded 16 mg (22%) of phenyl ether **13g** as yellow oil: <sup>1</sup>H NMR (300 MHz, CDCl<sub>3</sub>)  $\delta$  7.72 (d, 2H,  $J = 8.6$  Hz), 7.05 (s, 1H), 6.98 (d, 2H,  $J = 8.5$  Hz), 6.93–6.73 (m, 3H), 4.35 (q, 2H,  $J = 7.1$  Hz), 4.20 (s, 3H), 3.87 (s, 3H), 1.39 (t, 3H,  $J = 7.1$  Hz); LRMS (FAB)  $m/z$  371 ( $M + H^+$ ).

#### 4.1.26. Ethyl 3-(4-(3-chloro-4-methoxyphenoxy)phenyl)-1-methyl-1H-pyrazole-5-carboxylate (**13h**)

Phenyl ether **13h** was prepared from phenol **12** (30 mg, 0.12 mmol) by the procedure for **13b**, using 3-chloro-4-methoxyphenylboronic acid instead of phenylboronic acid. Purification of the residue via flash column chromatography on silica gel (EtOAc/*n*-hexane = 1:6) afforded 7 mg (15%) of phenyl ether **13h** as a colorless oil: <sup>1</sup>H NMR (300 MHz, CDCl<sub>3</sub>)  $\delta$  7.72 (d, 2H,  $J = 8.8$  Hz), 7.09 (d, 1H,  $J = 2.6$  Hz), 7.05 (s, 1H), 6.96 (d, 2H,  $J = 8.8$  Hz), 6.91–6.90 (m, 2H), 4.35 (q, 2H,  $J = 7.1$  Hz), 4.20 (s, 3H), 3.88 (s, 3H), 1.38 (t, 3H,  $J = 7.1$  Hz); LRMS (FAB)  $m/z$  387 ( $M + H^+$ ).

#### 4.1.27. Ethyl 1-methyl-3-(4-(4-(trifluoromethyl)phenoxy)phenyl)-1H-pyrazole-5-carboxylate (**13i**)

Phenyl ether **13i** was prepared from phenol **12** (30 mg, 0.12 mmol) by the procedure for **13b**, using 4-(trifluoromethyl)phenylboronic acid instead of phenylboronic acid. Purification of the residue via flash column chromatography on silica gel (EtOAc/*n*-hexane = 1:9) afforded 12 mg (26%) of phenyl ether **13i** as white solid with a melting point of 67–69 °C: <sup>1</sup>H NMR (300 MHz, CDCl<sub>3</sub>)  $\delta$  7.79 (d, 2H,  $J = 8.8$  Hz), 7.56 (d, 2H,  $J = 8.6$  Hz), 7.09–7.04 (m, 5H), 4.36 (q, 2H,  $J = 7.1$  Hz), 4.21 (s, 3H), 1.39 (t, 3H,  $J = 7.0$  Hz); LRMS (FAB)  $m/z$  391 ( $M + H^+$ ).

#### 4.1.28. Ethyl 3-(4-(4-(*tert*-butyl)phenoxy)phenyl)-1-methyl-1H-pyrazole-5-carboxylate (**13j**)

Phenyl ether **13j** was prepared from phenol **12** (30 mg, 0.12 mmol) by the procedure for **13b**, using 4-(*tert*-butyl)phenylboronic acid instead of phenylboronic acid. Purification of the residue via flash column chromatography on silica gel (EtOAc/*n*-hexane = 1:10) afforded 12 mg (26%) of phenyl ether **13j** as a colorless oil: FT-IR (thin film, neat)  $\nu_{\max}$  2960, 1724, 1507, 1442, 1242, 1119  $\text{cm}^{-1}$ ;  $^1\text{H}$  NMR (300 MHz,  $\text{CDCl}_3$ )  $\delta$  7.72 (d, 2H,  $J = 8.8$  Hz), 7.34 (d, 2H,  $J = 8.8$  Hz), 7.05 (s, 1H), 7.01 (d, 2H,  $J = 8.8$  Hz), 6.94 (d, 2H,  $J = 8.8$  Hz), 4.35 (q, 2H,  $J = 7.1$  Hz), 4.20 (s, 3H), 1.39 (t, 3H,  $J = 7.1$  Hz), 1.31 (s, 9H); LRMS (FAB)  $m/z$  379 ( $\text{M} + \text{H}^+$ ).

### 4.2. Synthesis of anilines for the carboxamide analogs

#### 4.2.1. 2-Butoxy-4-fluoro-1-nitrobenzene (**15**)

To a solution of 5-fluoro-2-nitrophenol **14** (1.0 g, 6.37 mmol) and triphenylphosphine (2.2 g, 8.28 mmol) in THF (20 mL) was added *n*-butanol (0.77 mL, 8.28 mmol) and diisopropylazodicarboxylate (1.63 mL, 0.11 8.28 mmol). The reaction mixture was stirred for 1 h at ambient temperature and quenched with  $\text{H}_2\text{O}$ . The reaction mixture was diluted with EtOAc. The organic layer was washed with water and brine, dried over  $\text{MgSO}_4$  and concentrated in vacuo. Purification of the residue via flash column chromatography on silica gel (EtOAc/*n*-hexane = 1:20) afforded 1.3 g (96%) of nitrophenol **15** as a yellow oil:  $^1\text{H}$  NMR (300 MHz,  $\text{CDCl}_3$ )  $\delta$  7.93–7.88 (m, 1H), 6.77–6.65 (m, 2H), 4.06 (t, 2H,  $J = 6.3$  Hz), 1.87–1.77 (m, 2H), 1.55–1.45 (m, 2H), 0.96 (t, 3H); LRMS (FAB)  $m/z$  214 ( $\text{M} + \text{H}^+$ ).

#### 4.2.2. 3-(3-Butoxy-4-nitrophenoxy)-*N,N*-diethylpropan-1-amine (**17a**)

To a solution of nitrophenol **15** (1.0 g, 1.41 mmol) and 3-diethylamino-1-propanol (0.77 mL, 5.16 mmol) in THF (10 mL) was added 60% NaH in mineral oil (281 mg, 2.12 mmol) at ambient temperature. The reaction mixture was refluxed for 24 h, concentrated in vacuo, and diluted with EtOAc. The organic phase was washed with water and brine, dried over  $\text{MgSO}_4$ , and concentrated in vacuo. Purification of the residue via flash column chromatography on silica gel (MeOH/ $\text{CH}_2\text{Cl}_2/\text{Et}_3\text{N} = 1:10:0.1$ ) afforded 880 mg (58%) of **17a** as yellow solid with a melting point of 35–38 °C: FT-IR (thin film, neat)  $\nu_{\max}$  2964, 2873, 1608, 1513, 1291, 1197  $\text{cm}^{-1}$ ;  $^1\text{H}$  NMR (300 MHz,  $\text{CDCl}_3$ )  $\delta$  7.93 (d, 2H,  $J = 9.0$  Hz), 6.49–6.44 (m, 2H), 4.08–4.03 (m, 4H), 2.62–2.51 (m, 6H), 1.95–1.77 (m, 4H), 1.55–1.48 (m, 2H), 1.04–0.94 (m, 9H); LRMS (ESI)  $m/z$  325 ( $\text{M} + \text{H}^+$ ).

#### 4.2.3. *N,N*-diethyl-3-(4-nitrophenoxy)propan-1-amine (**17b**)

Nitrobenzene **17b** was prepared from 4-nitrophenol **16** (2.5 g, 17.79 mmol) by the procedure for **15**, using 3-diethylamino-1-propanol instead of *n*-butanol. Purification of the residue via flash column chromatography on silica gel (MeOH/ $\text{CH}_2\text{Cl}_2 = 1:30$ ) afforded 4.0 g (89%) of nitrobenzene **17b** as a yellow oil:  $^1\text{H}$  NMR (300 MHz,  $\text{CDCl}_3$ )  $\delta$  8.17 (d, 2H,  $J = 9.2$  Hz), 6.93 (d, 2H,  $J = 9.2$  Hz), 4.09 (t, 2H,  $J = 6.3$  Hz), 2.60–2.48 (m, 6H), 2.02–1.89 (m, 2H), 1.00 (t, 6H,  $J = 7.1$  Hz); LRMS (FAB)  $m/z$  253 ( $\text{M} + \text{H}^+$ ).

#### 4.2.4. 2-Butoxy-4-(3-(diethylamino)propoxy)aniline (**18a**)

To a solution of nitrobenzene **17a** (880 mg, 2.71 mmol) in EtOH (20 mL) was added  $\text{SnCl}_2 \cdot 2\text{H}_2\text{O}$  (2.5 g, 10.84 mmol). The reaction mixture was refluxed for 3 h and concentrated in vacuo. The residue was diluted with EtOAc and saturated  $\text{NaHCO}_3$  solution was added. The mixture was filtered using a Celite pad. The organic phase was washed with water and brine, dried over  $\text{MgSO}_4$ , and concentrated in vacuo. Purification of the residue via flash column chromatography on silica gel (MeOH/ $\text{CH}_2\text{Cl}_2 = 1:10$ ) afforded 710 mg (89%) of aniline **18a** as a brown oil:  $^1\text{H}$  NMR (300 MHz,  $\text{CDCl}_3$ )  $\delta$  6.60 (d, 1H,

$J = 8.4$  Hz), 6.44–6.42 (m, 1H), 6.31 (dd, 1H,  $J = 2.8, 8.4$  Hz), 4.01–3.84 (m, 4H), 2.62–2.49 (m, 6H), 1.93–1.72 (m, 4H), 1.52–1.44 (m, 2H), 1.03–0.92 (m, 9H); LRMS (FAB)  $m/z$  295 ( $\text{M} + \text{H}^+$ ).

#### 4.2.5. 4-(3-(Diethylamino)propoxy)aniline (**18b**)

Aniline **18b** was prepared from nitrobenzene **17b** (2.0 g, 7.93 mmol) by the procedure for **18a**. Purification of the residue via flash column chromatography on silica gel (MeOH/ $\text{CH}_2\text{Cl}_2 = 1:10$ ) afforded 1.6 g (91%) of aniline **18b** as a brown oil:  $^1\text{H}$  NMR (300 MHz,  $\text{CDCl}_3$ )  $\delta$  7.02 (d, 2H,  $J = 7.9$  Hz), 6.31–6.22 (m, 3H), 3.94 (t, 2H,  $J = 6.4$  Hz), 3.61 (bs, 2H), 2.61–2.50 (m, 6H), 1.90 (q, 2H,  $J = 7.0$  Hz), 1.01 (t, 6H,  $J = 7.1$  Hz); LRMS (FAB)  $m/z$  223 ( $\text{M} + \text{H}^+$ ).

### 4.3. General synthetic procedure for the carboxamide analogs

To a solution of ethyl carboxylate (1 equiv) in THF/MeOH/ $\text{H}_2\text{O}$  (5:1:1) was added  $\text{LiOH} \cdot \text{H}_2\text{O}$  (10 equiv). The reaction mixture was stirred at ambient temperature until no starting material was observed by TLC. The reaction mixture was concentrated in vacuo, diluted with EtOAc, and acidified with 1 N HCl solution. The organic phase was washed with water and brine, dried over  $\text{MgSO}_4$ , and concentrated in vacuo. The residue was used for the next reaction without further purification. To a solution of above carboxylic acid (1 equiv) in  $\text{CH}_2\text{Cl}_2$  were added catalytic amount of DMF and oxalyl chloride (5 equiv) at 0 °C. The reaction mixture was stirred for 1 h at the same temperature, concentrated in vacuo, and diluted with THF. To a solution of above acid chloride were added aniline (1 equiv) and  $\text{Et}_3\text{N}$  (5 equiv). The reaction mixture was stirred for 1 h at ambient temperature, quenched with  $\text{H}_2\text{O}$ , and diluted with EtOAc. The organic phase was washed with water and brine, dried over  $\text{MgSO}_4$ , and concentrated in vacuo. Purification of the residue via flash column chromatography on silica gel (MeOH/ $\text{CH}_2\text{Cl}_2 = 1:10$ –20) afforded the desired carboxamide.

#### 4.3.1. *N*-(4-(2-(Diethylamino)ethoxy)phenyl)-3-(4-methoxyphenyl)-1-methyl-1H-pyrazole-5-carboxamide (**19**)

Carboxylate **7a** (15 mg, 0.06 mmol) afforded carboxamide **19** (13 mg, 53%) as white solid with a melting point of 133–136 °C: FT-IR (thin film, neat)  $\nu_{\max}$  3298, 2925, 1513, 1249  $\text{cm}^{-1}$ ;  $^1\text{H}$  NMR (300 MHz,  $\text{CD}_3\text{OD}$ )  $\delta$  7.72 (d, 2H,  $J = 8.8$  Hz), 7.57 (d, 2H,  $J = 9.0$  Hz), 7.17 (s, 1H), 6.97–6.93 (m, 4H), 4.16 (s, 3H), 4.12 (t, 2H,  $J = 5.6$  Hz), 3.82 (s, 3H), 3.00 (t, 2H,  $J = 5.6$  Hz), 2.76 (q, 4H,  $J = 7.2$  Hz), 1.13 (t, 6H,  $J = 7.1$  Hz);  $^{13}\text{C}$  NMR ( $\text{CDCl}_3$ , 75 MHz)  $\delta$  159.7, 158.0, 156.0, 149.7, 136.7, 130.2, 126.8, 126.8, 125.3, 122.2, 122.2, 115.1, 115.1, 114.2, 114.2, 102.5, 66.6, 55.3, 51.7, 47.8, 47.8, 39.4, 11.5, 11.5; LRMS (FAB)  $m/z$  423 ( $\text{M} + \text{H}^+$ ); HRMS (FAB) calcd for  $\text{C}_{24}\text{H}_{31}\text{N}_4\text{O}_3$  ( $\text{M} + \text{H}^+$ ): 423.2391; found 423.2396; HPLC (2.79 min, 97.9%).

#### 4.3.2. *N*-(4-(3-(Diethylamino)propoxy)phenyl)-3-(4-methoxyphenyl)-1-methyl-1H-pyrazole-5-carboxamide (**20**)

Carboxylate **7a** (15 mg, 0.06 mmol) afforded carboxamide **20** (18 mg, 71%) as a colorless oil:  $^1\text{H}$  NMR (300 MHz,  $\text{CD}_3\text{OD}$ )  $\delta$  7.72 (d, 2H,  $J = 9.0$  Hz), 7.57 (d, 2H,  $J = 9.0$  Hz), 7.17 (s, 1H), 6.97–6.91 (m, 4H), 4.15 (s, 3H), 4.05 (t, 2H,  $J = 5.9$  Hz), 3.81 (s, 3H), 3.02–2.88 (m, 6H), 2.08–2.00 (m, 2H), 1.20 (t, 6H,  $J = 7.2$  Hz);  $^{13}\text{C}$  NMR ( $\text{CDCl}_3$ , 100 MHz)  $\delta$  159.6, 158.1, 155.5, 149.6, 136.5, 130.8, 126.8, 126.8, 125.3, 122.4, 122.4, 114.8, 114.8, 114.1, 114.1, 103.1, 65.4, 55.3, 49.3, 46.7, 46.7, 39.4, 29.7, 9.3, 9.3; LRMS (FAB)  $m/z$  437 ( $\text{M} + \text{H}^+$ ); HRMS (FAB) calcd for  $\text{C}_{25}\text{H}_{33}\text{N}_4\text{O}_3$  ( $\text{M} + \text{H}^+$ ): 437.2547; found 437.2553; HPLC (2.83 min, 97.5%).

#### 4.3.3. *N*-(2-butoxy-4-(3-(diethylamino)propoxy)phenyl)-3-(4-methoxyphenyl)-1-methyl-1H-pyrazole-5-carboxamide (**21**)

Carboxylate **7a** (19 mg, 0.07 mmol) afforded carboxamide **21** (25 mg, 67%) as white solid with a melting point of 133–138 °C: FT-

IR (thin film, neat)  $\nu_{\max}$  3424, 2959, 1530, 1250  $\text{cm}^{-1}$ ;  $^1\text{H}$  NMR (300 MHz,  $\text{CDCl}_3$ )  $\delta$  8.26–8.23 (m, 2H), 7.67 (d, 2H,  $J = 8.8$  Hz), 6.92 (d, 2H,  $J = 8.8$  Hz), 6.72 (s, 1H), 6.47–6.43 (m, 2H), 4.21 (s, 3H), 4.07–3.99 (m, 4H), 3.81 (s, 3H), 3.57–3.43 (m, 4H), 2.99–2.87 (m, 2H), 2.31–2.14 (m, 2H), 1.88–1.78 (m, 2H), 1.60–1.47 (m, 2H), 1.35–1.12 (m, 6H), 1.00 (t, 3H,  $J = 7.3$  Hz);  $^{13}\text{C}$  NMR ( $\text{CDCl}_3$ , 75 MHz)  $\delta$  159.7, 157.3, 156.0, 149.7, 148.8, 137.2, 126.8, 126.8, 125.4, 121.1, 120.5, 114.2, 114.2, 105.0, 102.3, 100.0, 68.5, 66.3, 55.3, 49.4, 46.9, 46.9, 39.3, 31.2, 26.0, 19.4, 13.9, 10.7, 10.7; LRMS (FAB)  $m/z$  509 ( $\text{M} + \text{H}^+$ ); HRMS (FAB) calcd for  $\text{C}_{29}\text{H}_{41}\text{N}_4\text{O}_4$  ( $\text{M} + \text{H}^+$ ): 509.3122; found 509.3143; HPLC (4.04 min, 99.0%).

#### 4.3.4. *N*-(2-butoxy-4-(3-(diethylamino)propoxy)phenyl)-3-(4-methoxyphenyl)-1*H*-pyrazole-5-carboxamide (**22**)

Carboxylate **6a** (30 mg, 0.12 mmol) afforded carboxamide **22** (17 mg, 37%) as white solid with a melting point of 162–170 °C:  $^1\text{H}$  NMR (300 MHz,  $\text{CDCl}_3$ )  $\delta$  9.14 (s, 1H), 8.35 (d, 1H,  $J = 8.1$  Hz), 7.57 (d, 2H,  $J = 8.8$  Hz), 7.02 (s, 1H), 6.92 (d, 2H,  $J = 8.8$  Hz), 6.46–6.43 (m, 2H), 4.00–3.92 (m, 4H), 3.80 (s, 3H), 2.84–2.70 (m, 6H), 2.11–2.01 (m, 2H), 1.81–1.76 (m, 2H), 1.50 (q, 2H,  $J = 7.5$  Hz), 1.14 (t, 6H,  $J = 7.2$  Hz), 0.96 (t, 3H,  $J = 7.4$  Hz);  $^{13}\text{C}$  NMR ( $\text{CDCl}_3$ , 120 MHz)  $\delta$  160.0, 159.1, 157.8, 157.5, 155.3, 148.9, 126.9, 126.9, 121.8, 121.7, 120.4, 114.6, 114.6, 104.9, 102.3, 99.8, 71.4, 68.4, 55.4, 49.4, 46.8, 46.8, 31.2, 29.7, 19.2, 13.9, 10.4, 10.4; LRMS (FAB)  $m/z$  495 ( $\text{M} + \text{H}^+$ ); HRMS (FAB) calcd for  $\text{C}_{28}\text{H}_{39}\text{N}_4\text{O}_4$  ( $\text{M} + \text{H}^+$ ): 495.2966; found 495.2976; HPLC (3.66 min, 99.3%).

#### 4.3.5. 3-(4-(4-Chlorophenoxy)phenyl)-*N*-(4-(2-(diethylamino)ethoxy)phenyl)-1-methyl-1*H*-pyrazole-5-carboxamide (**23**)

Carboxylate **7c** (32 mg, 0.09 mmol) afforded carboxamide **23** (25 mg, 52%) as yellow solid with a melting point of 101–106 °C: FT-IR (thin film, neat)  $\nu_{\max}$  3298, 2969, 1512, 1486, 1241  $\text{cm}^{-1}$ ;  $^1\text{H}$  NMR (300 MHz,  $\text{CD}_3\text{OD}$ )  $\delta$  7.82 (d, 2H,  $J = 8.8$  Hz), 7.58 (d, 2H,  $J = 9.0$  Hz), 7.35 (d, 2H,  $J = 9.0$  Hz), 7.23 (s, 1H), 7.07–6.94 (m, 6H), 4.18 (s, 3H), 4.13–4.09 (m, 2H), 2.95–2.94 (m, 2H), 2.72 (q, 4H,  $J = 7.2$  Hz), 1.11 (t, 6H,  $J = 7.2$  Hz);  $^{13}\text{C}$  NMR ( $\text{CDCl}_3$ , 75 MHz)  $\delta$  157.8, 156.8, 156.1, 155.7, 149.1, 136.8, 130.1, 129.7, 129.7, 128.4, 128.1, 127.1, 127.1, 122.2, 122.2, 120.1, 120.1, 119.1, 119.1, 115.0, 115.0, 102.9, 66.6, 51.7, 47.8, 47.8, 39.4, 11.6, 11.6; LRMS (FAB)  $m/z$  519 ( $\text{M} + \text{H}^+$ ); HRMS (FAB) calcd for  $\text{C}_{29}\text{H}_{32}\text{ClN}_4\text{O}_3$  ( $\text{M} + \text{H}^+$ ): 519.2163; found 519.2176; HPLC (4.64 min, 99.8%).

#### 4.3.6. 3-(4-(4-Chlorophenoxy)phenyl)-*N*-(4-(3-(diethylamino)propoxy)phenyl)-1-methyl-1*H*-pyrazole-5-carboxamide (**24**)

Carboxylate **7c** (15 mg, 0.04 mmol) afforded carboxamide **24** (14 mg, 64%) as a brown oil:  $^1\text{H}$  NMR (300 MHz,  $\text{CD}_3\text{OD}$ )  $\delta$  7.80 (d, 2H,  $J = 8.8$  Hz), 7.56 (d, 2H,  $J = 9.0$  Hz), 7.34 (d, 2H,  $J = 8.8$  Hz), 7.21 (s, 1H), 7.04–6.90 (m, 6H), 4.15 (s, 3H), 4.02 (t, 2H,  $J = 5.9$  Hz), 2.91–2.77 (m, 6H), 2.10–1.98 (m, 2H), 1.15 (t, 6H,  $J = 7.2$  Hz);  $^{13}\text{C}$  NMR ( $\text{CDCl}_3$ , 100 MHz)  $\delta$  157.9, 156.9, 156.1, 155.8, 149.1, 136.8, 130.3, 129.8, 129.8, 128.4, 128.2, 127.1, 127.1, 122.3, 122.3, 120.1, 120.1, 119.1, 119.1, 114.9, 114.9, 103.0, 66.2, 50.8, 49.3, 46.8, 46.8, 39.5, 10.7, 10.7; LRMS (FAB)  $m/z$  533 ( $\text{M} + \text{H}^+$ ); HRMS (FAB) calcd for  $\text{C}_{30}\text{H}_{34}\text{ClN}_4\text{O}_3$  ( $\text{M} + \text{H}^+$ ): 533.2314; found 533.2319; HPLC (4.77 min, 95.3%).

#### 4.3.7. *N*-(2-butoxy-4-(3-(diethylamino)propoxy)phenyl)-3-(4-(4-chlorophenoxy)phenyl)-1-methyl-1*H*-pyrazole-5-carboxamide (**25**)

Carboxylate **7c** (34 mg, 0.10 mmol) afforded carboxamide **25** (35 mg, 60%) as pale yellow solid with a melting point of 70–74 °C: FT-IR (thin film, neat)  $\nu_{\max}$  3426, 2961, 1678, 1528, 1486, 1439, 1241  $\text{cm}^{-1}$ ;  $^1\text{H}$  NMR (300 MHz,  $\text{CD}_3\text{OD}$ )  $\delta$  7.81 (d, 2H,  $J = 8.4$  Hz), 7.61 (d, 2H,  $J = 9.0$  Hz), 7.35 (d, 2H,  $J = 8.8$  Hz), 7.15 (s, 1H), 7.06–6.99 (m, 4H), 6.63–6.53 (m, 3H), 4.17 (s, 3H), 4.05 (q, 4H,  $J = 5.4$  Hz), 2.96–2.82 (m, 6H), 2.06–2.01 (m, 2H), 1.82–1.75 (m, 2H), 1.56–1.48 (m, 2H), 1.18 (t, 6H,  $J = 7.1$  Hz), 0.96 (t, 3H,  $J = 7.4$  Hz);  $^{13}\text{C}$  NMR

( $\text{CDCl}_3$ , 75 MHz)  $\delta$  157.2, 156.9, 156.3, 155.8, 149.1, 148.8, 137.4, 129.8, 129.8, 128.4, 128.3, 127.1, 127.1, 120.7, 120.5, 120.1, 120.1, 119.1, 119.1, 104.9, 102.5, 100.0, 68.5, 66.8, 49.4, 47.0, 47.0, 39.4, 31.2, 27.1, 19.4, 13.9, 11.7, 11.7; LRMS (FAB)  $m/z$  605 ( $\text{M} + \text{H}^+$ ); HRMS (FAB) calcd for  $\text{C}_{34}\text{H}_{42}\text{ClN}_4\text{O}_4$  ( $\text{M} + \text{H}^+$ ): 605.2889; found 605.2883; HPLC (4.63 min, 97.7%).

#### 4.3.8. *N*-(2-butoxy-4-(3-(diethylamino)propoxy)phenyl)-3-(4-(4-chlorophenoxy)phenyl)-1*H*-pyrazole-5-carboxamide (**26**)

Carboxylate **6c** (33 mg, 0.10 mmol) afforded carboxamide **26** (25 mg, 46%) as white solid with a melting point of 137–142 °C:  $^1\text{H}$  NMR (300 MHz,  $\text{CD}_3\text{OD}$ )  $\delta$  8.15 (d, 1H,  $J = 8.1$  Hz), 7.72 (d, 2H,  $J = 8.8$  Hz), 7.37 (d, 2H,  $J = 9.0$  Hz), 7.10–7.01 (m, 5H), 6.64–6.53 (m, 2H), 4.11–4.06 (m, 4H), 3.01–2.86 (m, 6H), 2.03–2.00 (m, 2H), 1.86–1.83 (m, 2H), 1.64–1.60 (m, 2H), 1.19 (t, 6H,  $J = 6.5$  Hz), 1.02 (t, 3H,  $J = 7.3$  Hz);  $^{13}\text{C}$  NMR ( $\text{CDCl}_3$ , 75 MHz)  $\delta$  157.7, 156.8, 155.9, 151.9, 148.9, 138.5, 133.8, 129.0, 129.0, 127.2, 127.2, 126.2, 126.2, 126.0, 123.6, 121.0, 120.6, 116.0, 116.0, 105.7, 104.5, 99.6, 68.4, 65.8, 48.9, 46.2, 46.2, 31.0, 25.0, 19.3, 13.9, 9.7, 9.7; LRMS (FAB)  $m/z$  591 ( $\text{M} + \text{H}^+$ ); HRMS (FAB) calcd for  $\text{C}_{33}\text{H}_{40}\text{ClN}_4\text{O}_4$  ( $\text{M} + \text{H}^+$ ): 591.2733; found 591.2738; HPLC (2.80 min, 98.8%).

#### 4.3.9. *N*-(2-butoxy-4-(3-(diethylamino)propoxy)phenyl)-3-(4-(4-chlorophenoxy)phenyl)isoxazole-5-carboxamide (**27**)

Carboxylate **8** (25 mg, 0.073 mmol) afforded the carboxamide **27** (17 mg, 38%) as white solid with a melting point of 135–138 °C: FT-IR (thin film, neat)  $\nu_{\max}$  3383, 2959, 1685, 1543, 1486, 1247, 1178  $\text{cm}^{-1}$ ;  $^1\text{H}$  NMR (300 MHz,  $\text{CD}_3\text{OD}$ )  $\delta$  8.01 (d, 1H,  $J = 8.8$  Hz), 7.81 (d, 2H,  $J = 9.0$  Hz), 7.31 (d, 2H,  $J = 9.0$  Hz), 7.04–6.95 (m, 5H), 6.57 (d, 1H,  $J = 2.6$  Hz), 6.47 (dd, 1H,  $J = 2.6, 8.8$  Hz), 4.02–3.98 (m, 4H), 3.13–2.99 (m, 6H), 2.09–2.02 (m, 2H), 1.81–1.71 (m, 2H), 1.55–1.42 (m, 2H), 1.19 (t, 6H,  $J = 7.3$  Hz), 0.93 (t, 3H,  $J = 7.4$  Hz);  $^{13}\text{C}$  NMR ( $\text{CDCl}_3$ , 75 MHz)  $\delta$  171.1, 159.8, 159.3, 156.1, 155.7, 154.5, 149.1, 130.0, 130.0, 129.4, 127.8, 127.8, 121.9, 121.0, 121.0, 121.0, 120.7, 118.6, 118.6, 104.8, 99.8, 98.5, 68.6, 65.6, 49.3, 46.8, 46.8, 31.1, 24.8, 19.2, 13.8, 9.5, 9.5; LRMS (FAB)  $m/z$  592 ( $\text{M} + \text{H}^+$ ); HRMS (FAB) calcd for  $\text{C}_{33}\text{H}_{39}\text{ClN}_3\text{O}_5$  ( $\text{M} + \text{H}^+$ ): 592.2573; found 592.2585; HPLC (10.57 min, 95.1%).

#### 4.3.10. *N*-(2-butoxy-4-(3-(diethylamino)propoxy)phenyl)-3-(4-(4-chlorophenoxy)phenyl)-1-ethyl-1*H*-pyrazole-5-carboxamide (**28**)

Carboxylate **9** (19 mg, 0.051 mmol) afforded carboxamide **28** (21 mg, 67%) as a yellow oil:  $^1\text{H}$  NMR (300 MHz,  $\text{CD}_3\text{OD}$ )  $\delta$  7.81 (d, 2H,  $J = 8.6$  Hz), 7.59 (d, 1H,  $J = 8.6$  Hz), 7.35–7.32 (m, 2H), 7.12 (s, 1H), 7.05–6.98 (m, 4H), 6.63 (d, 1H,  $J = 2.4$  Hz), 6.54 (dd, 1H,  $J = 2.6, 8.8$  Hz), 4.60–4.56 (m, 2H), 4.08–4.01 (m, 4H), 3.08–2.94 (m, 6H), 2.12–2.03 (m, 2H), 1.80–1.75 (m, 2H), 1.54–1.41 (m, 5H), 1.22 (t, 6H,  $J = 7.2$  Hz), 0.95 (t, 3H,  $J = 7.3$  Hz);  $^{13}\text{C}$  NMR ( $\text{CDCl}_3$ , 75 MHz)  $\delta$  157.1, 156.8, 155.9, 155.8, 149.2, 148.9, 136.6, 129.8, 129.8, 128.5, 128.4, 127.1, 127.1, 121.1, 120.6, 120.1, 120.1, 119.2, 119.2, 105.0, 102.6, 99.9, 68.5, 66.0, 49.2, 47.0, 46.8, 46.8, 31.2, 25.4, 19.4, 16.0, 13.9, 10.1, 10.1; LRMS (FAB)  $m/z$  619 ( $\text{M} + \text{H}^+$ ); HRMS (FAB) calcd for  $\text{C}_{35}\text{H}_{44}\text{ClN}_4\text{O}_4$  ( $\text{M} + \text{H}^+$ ): 619.3046; found 619.3048; HPLC (5.12 min, 95.2%).

#### 4.3.11. *N*-(2-butoxy-4-(3-(diethylamino)propoxy)phenyl)-3-(4-(4-chlorophenoxy)phenyl)-1-propyl-1*H*-pyrazole-5-carboxamide (**29**)

Carboxylate **10** (27 mg, 0.07 mmol) afforded carboxamide **29** (21 mg, 47%) as a colorless oil:  $^1\text{H}$  NMR (300 MHz,  $\text{CD}_3\text{OD}$ )  $\delta$  7.82 (d, 2H,  $J = 8.8$  Hz), 7.57 (d, 1H,  $J = 8.6$  Hz), 7.36–7.32 (m, 2H), 7.14 (s, 1H), 7.06–6.99 (m, 4H), 6.62 (d, 1H,  $J = 2.6$  Hz), 6.53 (dd, 1H,  $J = 2.6, 8.6$  Hz), 4.53 (t, 2H,  $J = 7.1$  Hz), 4.06–4.01 (m, 4H), 2.88–2.83 (m, 2H), 2.78 (q, 4H,  $J = 7.1$  Hz), 2.03–1.96 (m, 2H), 1.93–1.86 (m, 2H), 1.80–1.73 (m, 2H), 1.54–1.47 (m, 2H), 1.14 (t, 6H,  $J = 7.1$  Hz), 0.94 (q, 6H,  $J = 7.5$  Hz);  $^{13}\text{C}$  NMR ( $\text{CDCl}_3$ , 150 MHz)  $\delta$  157.2, 156.8, 156.0, 155.9, 149.1, 148.8, 137.1, 129.8, 129.8, 128.5, 128.3, 127.1, 127.1, 120.9,

120.5, 120.0, 120.0, 119.2, 119.2, 104.9, 102.6, 99.9, 68.5, 66.4, 53.2, 49.3, 46.9, 46.9, 31.2, 26.2, 24.2, 19.4, 13.9, 11.1, 10.9, 10.9; LRMS (FAB)  $m/z$  633 (M + H<sup>+</sup>); HRMS (FAB) calcd for C<sub>36</sub>H<sub>46</sub>ClN<sub>4</sub>O<sub>4</sub> (M + H<sup>+</sup>): 633.3202; found 633.3207; HPLC (9.04 min, 99.3%).

#### 4.3.12. *N*-(2-butoxy-4-(3-(diethylamino)propoxy)phenyl)-5-(4-(4-chlorophenoxy)phenyl)-1-propyl-1H-pyrazole-3-carboxamide (**30**)

Carboxylate **10'** (12 mg, 0.03 mmol) afforded carboxamide **30** (10 mg, 51%) as a pale yellow oil: <sup>1</sup>H NMR (300 MHz, CD<sub>3</sub>OD) δ 8.19 (d, 1H, *J* = 8.8 Hz), 7.44 (d, 2H, *J* = 8.6 Hz), 7.38 (d, 2H, *J* = 9.0 Hz), 7.10 (d, 2H, *J* = 8.8 Hz), 7.04 (d, 2H, *J* = 9.0 Hz), 6.77 (s, 1H), 6.60–6.49 (m, 2H), 4.16–4.05 (m, 4H), 4.00 (t, 2H, *J* = 6.0 Hz), 2.77–2.63 (m, 6H), 1.99–1.79 (m, 6H), 1.66–1.62 (m, 2H), 1.10 (t, 6H, *J* = 7.1 Hz), 1.03 (t, 3H, *J* = 7.5 Hz), 0.85 (t, 3H, *J* = 7.3 Hz); <sup>13</sup>C NMR (CDCl<sub>3</sub>, 75 MHz) δ 159.5, 157.9, 155.5, 155.0, 148.9, 146.3, 144.8, 130.6, 130.6, 130.0, 130.0, 129.2, 125.3, 121.9, 120.8, 120.8, 120.1, 118.5, 118.5, 106.6, 104.9, 100.1, 68.3, 66.6, 51.6, 49.5, 47.0, 47.0, 31.4, 26.8, 23.4, 19.4, 13.9, 11.5, 11.5, 11.1; LRMS (FAB)  $m/z$  633 (M + H<sup>+</sup>); HRMS (FAB) calcd for C<sub>36</sub>H<sub>46</sub>ClN<sub>4</sub>O<sub>4</sub> (M + H<sup>+</sup>): 633.3202; found 633.3192; HPLC (11.24 min, 97.2%).

#### 4.3.13. *N*-(2-butoxy-4-(3-(diethylamino)propoxy)phenyl)-1-butyl-5-(4-(4-chlorophenoxy)phenyl)-1H-pyrazole-3-carboxamide (**31**)

Carboxylate **11'** (62 mg, 0.16 mmol) afforded carboxamide **31** (48 mg, 47%) as pale yellow solid with a melting point of 137–145 °C: FT-IR (thin film, neat)  $\nu_{\max}$  3383, 2959, 1677, 1536, 1484, 1243 cm<sup>-1</sup>; <sup>1</sup>H NMR (300 MHz, CD<sub>3</sub>OD) δ 8.20 (d, 1H, *J* = 8.8 Hz), 7.48 (d, 2H, *J* = 8.8 Hz), 7.39 (d, 2H, *J* = 9.0 Hz), 7.13 (d, 2H, *J* = 8.6 Hz), 7.06 (d, 2H, *J* = 9.2 Hz), 6.79 (s, 1H), 6.64 (d, 1H, *J* = 2.6 Hz), 6.53 (dd, 1H, *J* = 2.4, 8.8 Hz), 4.21 (t, 2H, *J* = 7.2 Hz), 4.13–4.06 (m, 4H), 2.89–2.74 (m, 6H), 2.06–2.01 (m, 2H), 1.86–1.81 (m, 4H), 1.70–1.62 (m, 2H), 1.30–1.25 (m, 2H), 1.14 (t, 6H, *J* = 7.2 Hz), 1.04 (t, 3H, *J* = 7.3 Hz), 0.87 (t, 3H, *J* = 7.4 Hz); <sup>13</sup>C NMR (CDCl<sub>3</sub>, 75 MHz) δ 157.2, 156.8, 155.9, 155.9, 149.1, 148.9, 137.0, 129.7, 129.7, 128.5, 128.3, 127.1, 127.1, 121.1, 120.6, 120.0, 120.0, 119.2, 119.2, 105.0, 102.6, 99.9, 68.5, 66.1, 51.5, 49.3, 46.9, 46.9, 32.9, 31.2, 25.6, 19.9, 19.4, 13.9, 13.7, 10.3, 10.3; LRMS (FAB)  $m/z$  647 (M + H<sup>+</sup>); HRMS (FAB) calcd for C<sub>37</sub>H<sub>48</sub>ClN<sub>4</sub>O<sub>4</sub> (M + H<sup>+</sup>): 647.3359; found 647.3359; HPLC (7.34 min, 95.8%).

#### 4.3.14. *N*-(2-butoxy-4-(3-(diethylamino)propoxy)phenyl)-1-butyl-3-(4-(4-chlorophenoxy)phenyl)-1H-pyrazole-5-carboxamide (**32**)

Carboxylate **11** (33 mg, 0.08 mmol) afforded carboxamide **32** (23 mg, 44%) as white solid with a melting point of 102–107 °C: FT-IR (thin film, neat)  $\nu_{\max}$  3424, 2959, 1675, 1527, 1485, 1241 cm<sup>-1</sup>; <sup>1</sup>H NMR (300 MHz, CD<sub>3</sub>OD) δ 7.82 (d, 2H, *J* = 8.6 Hz), 7.56 (d, 1H, *J* = 8.6 Hz), 7.37–7.32 (m, 2H), 7.13 (bs, 1H), 7.06–6.98 (m, 4H), 6.63 (d, 1H, *J* = 2.6 Hz), 6.53 (dd, 1H, *J* = 2.6, 8.8 Hz), 4.57 (t, 2H, *J* = 7.2 Hz), 4.06–4.01 (m, 4H), 2.76–2.62 (m, 6H), 1.95–1.74 (m, 6H), 1.55–1.45 (m, 2H), 1.40–1.32 (m, 2H), 1.12–1.06 (m, 6H), 0.98–0.92 (m, 6H); <sup>13</sup>C NMR (CDCl<sub>3</sub>, 75 MHz) δ 159.5, 157.8, 155.0, 155.0, 148.9, 146.1, 144.7, 130.6, 130.6, 129.9, 129.9, 129.1, 125.1, 122.0, 120.7, 120.7, 119.9, 118.5, 118.5, 106.5, 104.7, 99.8, 68.3, 65.9, 49.7, 49.3, 46.8, 46.8, 32.1, 31.3, 25.4, 19.7, 19.3, 13.9, 13.5, 10.2, 10.2; LRMS (FAB)  $m/z$  647 (M + H<sup>+</sup>); HRMS (FAB) calcd for C<sub>37</sub>H<sub>48</sub>ClN<sub>4</sub>O<sub>4</sub> (M + H<sup>+</sup>): 647.3359; found 647.3364; HPLC (10.97 min, 87.8%).

#### 4.3.15. 1-Butyl-3-(4-(4-chlorophenoxy)phenyl)-*N*-(4-(3-(diethylamino)propoxy)phenyl)-1H-pyrazole-5-carboxamide (**33**)

Carboxylate **11** (33 mg, 0.08 mmol) afforded carboxamide **33** (21 mg, 45%) as a pale yellow oil: <sup>1</sup>H NMR (300 MHz, CD<sub>3</sub>OD) δ 7.82 (d, 2H, *J* = 8.8 Hz), 7.58 (d, 2H, *J* = 9.0 Hz), 7.35 (d, 2H, *J* = 9.0 Hz), 7.21 (s, 1H), 7.06–6.93 (m, 6H), 4.57 (t, 2H, *J* = 7.1 Hz), 4.07 (t, 2H, *J* = 5.8 Hz), 3.11–2.92 (m, 6H), 2.14–2.05 (m, 2H), 1.90–1.80 (m, 2H), 1.42–1.20 (m, 8H), 0.95 (t, 3H, *J* = 7.3 Hz); <sup>13</sup>C NMR (CDCl<sub>3</sub>,

125 MHz) δ 157.8, 156.8, 156.0, 155.8, 149.1, 136.4, 130.3, 129.8, 129.8, 128.4, 128.4, 127.2, 127.2, 122.3, 122.3, 120.1, 120.1, 119.2, 119.2, 114.9, 114.9, 103.0, 66.0, 51.6, 49.3, 46.8, 46.8, 32.9, 29.7, 19.9, 13.7, 10.5, 10.5; LRMS (FAB)  $m/z$  575 (M + H<sup>+</sup>); HRMS (FAB) calcd for C<sub>33</sub>H<sub>40</sub>ClN<sub>4</sub>O<sub>3</sub> (M + H<sup>+</sup>): 575.2783; found 575.2789; HPLC (4.45 min, 95.1%).

#### 4.3.16. *N*-(2-butoxy-4-(3-(diethylamino)propoxy)phenyl)-3-(4-(cyclohexyloxy)phenyl)-1-methyl-1H-pyrazole-5-carboxamide (**34**)

Carboxylate **13a** (20 mg, 0.06 mmol) afforded carboxamide **34** (23 mg, 65%) as white solid with a melting point of 118–124 °C: <sup>1</sup>H NMR (300 MHz, CD<sub>3</sub>OD) δ 7.69–7.62 (m, 3H), 7.04 (s, 1H), 6.93 (d, 2H, *J* = 8.8 Hz), 6.60 (d, 1H, *J* = 2.3 Hz), 6.52 (dd, 1H, *J* = 2.4, 8.6 Hz), 4.35–4.32 (m, 1H), 4.13 (s, 3H), 4.02 (t, 4H, *J* = 6.0 Hz), 2.91–2.78 (m, 6H), 2.10–1.99 (m, 4H), 1.86–1.78 (m, 4H), 1.55–1.39 (m, 8H), 1.16 (t, 6H, *J* = 7.1 Hz), 0.97 (t, 3H, *J* = 7.3 Hz); <sup>13</sup>C NMR (CDCl<sub>3</sub>, 75 MHz) δ 157.8, 157.3, 155.9, 149.7, 148.7, 137.1, 126.7, 126.7, 125.0, 120.9, 120.4, 116.2, 116.2, 104.7, 102.2, 99.8, 75.4, 68.4, 66.2, 49.3, 46.8, 46.8, 39.3, 31.8, 31.8, 31.1, 26.0, 25.6, 23.7, 23.7, 19.4, 13.9, 10.7, 10.7; LRMS (FAB)  $m/z$  577 (M + H<sup>+</sup>); HRMS (FAB) calcd for C<sub>34</sub>H<sub>49</sub>N<sub>4</sub>O<sub>4</sub> (M + H<sup>+</sup>): 577.3754; found 577.3748; HPLC (4.83 min, 98.0%).

#### 4.3.17. *N*-(2-butoxy-4-(3-(diethylamino)propoxy)phenyl)-1-methyl-3-(4-phenoxyphenyl)-1H-pyrazole-5-carboxamide (**35**)

Carboxylate **13b** (18 mg, 0.06 mmol) afforded carboxamide **35** (20 mg, 63%) as pale yellow solid with a melting point of 69–72 °C: FT-IR (thin film, neat)  $\nu_{\max}$  3425, 2960, 1676, 1528, 1439, 1240 cm<sup>-1</sup>; <sup>1</sup>H NMR (300 MHz, CD<sub>3</sub>OD) δ 7.77 (d, 2H, *J* = 8.6 Hz), 7.62 (d, 1H, *J* = 8.8 Hz), 7.38–7.33 (m, 2H), 7.14–7.10 (m, 2H), 7.03–6.99 (m, 4H), 6.61 (d, 1H, *J* = 2.6 Hz), 6.52 (dd, 1H, *J* = 2.6, 8.6 Hz), 4.15 (s, 3H), 4.05–4.00 (m, 4H), 2.96–2.82 (m, 6H), 2.07–2.00 (m, 2H), 1.83–1.73 (m, 2H), 1.56–1.44 (m, 2H), 1.17 (t, 6H, *J* = 7.2 Hz), 0.95 (t, 3H, *J* = 7.4 Hz); <sup>13</sup>C NMR (CDCl<sub>3</sub>, 125 MHz) δ 157.3, 157.2, 157.1, 156.0, 149.3, 148.8, 137.3, 129.8, 129.8, 127.8, 127.0, 127.0, 123.4, 120.9, 120.4, 119.1, 119.1, 119.0, 119.0, 104.8, 102.5, 99.9, 68.5, 66.3, 49.3, 46.9, 46.9, 39.4, 31.2, 26.2, 19.4, 13.9, 10.9, 10.9; LRMS (FAB)  $m/z$  571 (M + H<sup>+</sup>); HRMS (FAB) calcd for C<sub>34</sub>H<sub>43</sub>N<sub>4</sub>O<sub>4</sub> (M + H<sup>+</sup>): 571.3279; found 571.3284; HPLC (6.02 min, 97.3%).

#### 4.3.18. *N*-(2-butoxy-4-(3-(diethylamino)propoxy)phenyl)-1-methyl-3-(4-(pyridin-2-yloxy)phenyl)-1H-pyrazole-5-carboxamide (**36**)

Carboxylate **7d** (30 mg, 0.09 mmol) afforded carboxamide **36** (22 mg, 42%) as a colorless oil: FT-IR (thin film, neat)  $\nu_{\max}$  3423, 2957, 1674, 1528, 1429, 1244 cm<sup>-1</sup>; <sup>1</sup>H NMR (300 MHz, CD<sub>3</sub>OD) δ 8.15–8.13 (m, 1H), 7.87–7.78 (m, 3H), 7.62 (d, 1H, *J* = 8.8 Hz), 7.16–6.09 (m, 4H), 6.97 (d, 1H, *J* = 8.3 Hz), 6.62 (d, 1H, *J* = 2.6 Hz), 6.53 (dd, 1H, *J* = 2.4, 8.6 Hz), 4.17 (s, 3H), 4.12–4.01 (m, 4H), 3.02–2.88 (m, 6H), 2.10–2.02 (m, 2H), 1.84–1.74 (m, 2H), 1.58–1.45 (m, 2H), 1.20 (t, 6H, *J* = 7.2 Hz), 0.96 (t, 3H, *J* = 7.4 Hz); <sup>13</sup>C NMR (CDCl<sub>3</sub>, 75 MHz) δ 163.7, 157.2, 155.9, 154.1, 149.3, 148.8, 147.8, 139.5, 137.3, 129.2, 126.9, 126.9, 121.4, 121.4, 121.0, 120.5, 118.6, 111.7, 104.9, 102.7, 99.9, 68.5, 66.2, 53.0, 49.3, 46.9, 46.9, 39.4, 31.2, 19.4, 13.9, 10.6, 10.6; LRMS (FAB)  $m/z$  572 (M + H<sup>+</sup>); HRMS (FAB) calcd for C<sub>33</sub>H<sub>42</sub>N<sub>5</sub>O<sub>4</sub> (M + H<sup>+</sup>): 572.3237; found 572.3231; HPLC (3.17 min, 97.4%).

#### 4.3.19. *N*-(2-butoxy-4-(3-(diethylamino)propoxy)phenyl)-3-(4-(4-methoxyphenoxy)phenyl)-1-methyl-1H-pyrazole-5-carboxamide (**37**)

Carboxylate **13c** (17 mg, 0.05 mmol) afforded carboxamide **37** (22 mg, 76%) as white solid with a melting point of 97–100 °C: <sup>1</sup>H NMR (300 MHz, CD<sub>3</sub>OD) δ 7.71 (d, 2H, *J* = 8.6 Hz), 7.64 (d, 1H, *J* = 8.8 Hz), 7.07 (s, 1H), 6.99–6.90 (m, 6H), 6.60 (d, 1H, *J* = 2.4 Hz), 6.51 (dd, 1H, *J* = 2.6, 8.8 Hz), 4.14 (s, 3H), 4.05–4.00 (m, 4H), 3.78 (s, 3H), 2.96–2.82 (m, 6H), 2.07–1.98 (m, 2H), 1.83–1.73 (m, 2H), 1.57–

1.44 (m, 2H), 1.17 (t, 6H,  $J = 7.2$  Hz), 0.95 (t, 3H,  $J = 7.4$  Hz);  $^{13}\text{C}$  NMR ( $\text{CDCl}_3$ , 75 MHz)  $\delta$  158.5, 157.2, 156.0, 155.9, 149.9, 149.3, 138.8, 137.2, 127.1, 126.9, 126.9, 120.9, 120.8, 120.8, 120.4, 117.8, 117.8, 114.9, 114.9, 104.8, 102.4, 99.9, 68.5, 66.3, 55.7, 49.3, 46.9, 46.9, 39.4, 31.2, 26.1, 19.4, 13.9, 10.8, 10.8; LRMS (FAB)  $m/z$  601 ( $\text{M} + \text{H}^+$ ); HRMS (FAB) calcd for  $\text{C}_{35}\text{H}_{45}\text{N}_4\text{O}_5$  ( $\text{M} + \text{H}^+$ ): 601.3390; found 601.3384; HPLC (3.78 min, 97.3%).

4.3.20. *N*-(2-butoxy-4-(3-(diethylamino)propoxy)phenyl)-3-(4-(4-(tert-butyl)phenoxy)phenyl)-1-methyl-1H-pyrazole-5-carboxamide (**38**)

Carboxylate **13j** (11 mg, 0.03 mmol) afforded carboxamide **38** (12 mg, 66%) as a pale yellow oil: FT-IR (thin film, neat)  $\nu_{\text{max}}$  3424, 2927, 1736, 1528, 1242  $\text{cm}^{-1}$ ;  $^1\text{H}$  NMR (300 MHz,  $\text{CD}_3\text{OD}$ )  $\delta$  7.75 (d, 2H,  $J = 8.6$  Hz), 7.63 (d, 1H,  $J = 8.8$  Hz), 7.40 (d, 2H,  $J = 8.6$  Hz), 7.12 (s, 1H), 7.00–6.93 (m, 4H), 6.64 (d, 1H,  $J = 2.4$  Hz), 6.54 (dd, 1H,  $J = 2.8$ , 8.8 Hz), 4.15 (s, 3H), 4.13–4.02 (m, 4H), 3.41–3.10 (m, 6H), 2.18–2.10 (m, 2H), 1.84–1.74 (m, 2H), 1.55–1.45 (m, 2H), 1.32–1.26 (m, 15H), 0.96 (t, 3H,  $J = 7.3$  Hz);  $^{13}\text{C}$  NMR ( $\text{CDCl}_3$ , 75 MHz)  $\delta$  157.6, 157.2, 155.9, 154.5, 149.4, 148.8, 146.3, 137.2, 127.5, 126.9, 126.9, 126.6, 126.6, 121.0, 120.4, 118.8, 118.8, 118.4, 118.4, 104.8, 102.5, 99.8, 68.5, 66.1, 49.2, 46.7, 46.7, 39.4, 34.3, 31.5, 31.5, 31.5, 31.1, 25.6, 19.4, 13.9, 10.4, 10.4; LRMS (FAB)  $m/z$  627 ( $\text{M} + \text{H}^+$ ); HRMS (FAB) calcd for  $\text{C}_{38}\text{H}_{51}\text{N}_4\text{O}_4$  ( $\text{M} + \text{H}^+$ ): 627.3905; found 627.3918; HPLC (6.58 min, 99.2%).

4.3.21. *N*-(2-butoxy-4-(3-(diethylamino)propoxy)phenyl)-1-methyl-3-(4-(4-(trifluoromethyl)phenoxy)phenyl)-1H-pyrazole-5-carboxamide (**39**)

Carboxylate **13i** (11 mg, 0.03 mmol) afforded the carboxamide **39** (12 mg, 68%) as pale yellow solid with a melting point of 123–129 °C:  $^1\text{H}$  NMR (300 MHz,  $\text{CD}_3\text{OD}$ )  $\delta$  7.86 (d, 2H,  $J = 8.6$  Hz), 7.67–7.60 (m, 3H), 7.18–7.11 (m, 5H), 7.64 (d, 1H,  $J = 2.4$  Hz), 6.55 (dd, 1H,  $J = 2.6$ , 8.8 Hz), 4.18 (s, 3H), 4.09–4.03 (m, 4H), 3.05–2.91 (m, 6H), 2.11–2.00 (m, 2H), 1.80–1.76 (m, 2H), 1.54–1.50 (m, 2H), 1.21 (t, 6H,  $J = 7.2$  Hz), 0.97 (t, 3H,  $J = 7.4$  Hz);  $^{13}\text{C}$  NMR ( $\text{CDCl}_3$ , 75 MHz)  $\delta$  160.3, 157.1, 155.8, 155.7, 149.0, 148.8, 137.4, 129.1, 127.2, 127.2, 127.2, 127.2, 127.1, 127.1, 121.0, 120.5, 120.1, 120.1, 118.0, 118.0, 104.9, 102.6, 99.8, 68.5, 66.0, 49.3, 46.8, 46.8, 39.5, 31.2, 19.4, 15.3, 13.9, 10.2, 10.2; LRMS (FAB)  $m/z$  639 ( $\text{M} + \text{H}^+$ ); HRMS (FAB) calcd for  $\text{C}_{35}\text{H}_{42}\text{F}_3\text{N}_4\text{O}_4$  ( $\text{M} + \text{H}^+$ ): 639.3158; found 639.3153; HPLC (4.50 min, 98.8%).

4.3.22. *N*-(2-butoxy-4-(3-(diethylamino)propoxy)phenyl)-3-(4-(4-fluorophenoxy)phenyl)-1-methyl-1H-pyrazole-5-carboxamide (**40**)

Carboxylate **13d** (29 mg, 0.09 mmol) afforded carboxamide **40** (33 mg, 67%) as pale yellow solid with a melting point of 133–138 °C: FT-IR (thin film, neat)  $\nu_{\text{max}}$  3424, 2928, 1737, 1675, 1528, 1500, 1249, 1214  $\text{cm}^{-1}$ ;  $^1\text{H}$  NMR (300 MHz,  $\text{CD}_3\text{OD}$ )  $\delta$  7.67 (d, 2H,  $J = 8.6$  Hz), 7.53 (d, 1H,  $J = 8.6$  Hz), 7.03–6.80 (m, 7H), 6.52 (d, 1H,  $J = 2.4$  Hz), 6.43 (dd, 1H,  $J = 2.6$ , 8.8 Hz), 4.15 (s, 3H), 3.97–3.91 (m, 4H), 2.88–2.74 (m, 6H), 1.99–1.91 (m, 2H), 1.73–1.64 (m, 2H), 1.47–1.35 (m, 2H), 1.09 (t, 6H,  $J = 7.2$  Hz), 0.86 (t, 3H,  $J = 7.4$  Hz);  $^{13}\text{C}$  NMR ( $\text{CDCl}_3$ , 75 MHz)  $\delta$  160.2, 157.4, 157.0, 156.9, 155.9, 148.9, 148.6, 137.0, 127.6, 126.8, 126.8, 120.6, 120.4, 120.3, 120.3, 118.2, 118.2, 116.3, 116.0, 104.6, 102.3, 99.7, 68.2, 66.2, 49.1, 46.8, 46.8, 29.2, 31.0, 26.2, 19.2, 13.7, 11.0, 11.0; LRMS (FAB)  $m/z$  589 ( $\text{M} + \text{H}^+$ ); HRMS (FAB) calcd for  $\text{C}_{34}\text{H}_{42}\text{FN}_4\text{O}_4$  ( $\text{M} + \text{H}^+$ ): 589.3185; found 589.3190; HPLC (4.07 min, 99.4%).

4.3.23. *N*-(2-butoxy-4-(3-(diethylamino)propoxy)phenyl)-3-(4-(3-fluorophenoxy)phenyl)-1-methyl-1H-pyrazole-5-carboxamide (**41**)

Carboxylate **13e** (24 mg, 0.07 mmol) afforded carboxamide **41** (20 mg, 48%) as yellow solid with a melting point of 156–161 °C: FT-IR (thin film, neat)  $\nu_{\text{max}}$  3425, 2960, 1675, 1528, 1439, 1216  $\text{cm}^{-1}$ ;  $^1\text{H}$  NMR (300 MHz,  $\text{CD}_3\text{OD}$ )  $\delta$  7.81 (d, 2H,  $J = 8.6$  Hz), 7.65 (d, 1H,

$J = 8.6$  Hz), 7.37–7.30 (m, 1H), 7.12 (s, 1H), 7.06 (d, 2H,  $J = 8.8$  Hz), 6.87–6.72 (m, 3H), 6.61 (d, 1H,  $J = 2.4$  Hz), 6.52 (dd, 1H,  $J = 2.6$ , 8.6 Hz), 4.15 (s, 3H), 4.02 (t, 4H,  $J = 6.0$  Hz), 2.90–2.76 (m, 6H), 2.10–1.99 (m, 2H), 1.80–1.75 (m, 2H), 1.50 (q, 2H,  $J = 7.5$  Hz), 1.15 (t, 6H,  $J = 7.2$  Hz), 0.96 (t, 3H,  $J = 7.4$  Hz);  $^{13}\text{C}$  NMR ( $\text{CDCl}_3$ , 75 MHz)  $\delta$  165.2, 161.9, 157.2, 156.3, 156.0, 149.1, 148.9, 137.4, 130.7, 128.7, 127.2, 127.2, 121.0, 120.6, 119.7, 119.7, 114.1, 110.2, 106.3, 105.0, 102.6, 100.0, 68.6, 66.3, 49.4, 46.9, 46.9, 39.4, 31.2, 26.1, 19.4, 13.9, 10.7, 10.7; LRMS (FAB)  $m/z$  589 ( $\text{M} + \text{H}^+$ ); HRMS (FAB) calcd for  $\text{C}_{34}\text{H}_{42}\text{FN}_4\text{O}_4$  ( $\text{M} + \text{H}^+$ ): 589.3190; found 589.3184; HPLC (6.12 min, 98.2%).

4.3.24. *N*-(2-butoxy-4-(2-(diethylamino)propoxy)phenyl)-3-(4-(3-fluorophenoxy)phenyl)-1-methyl-1H-pyrazole-5-carboxamide (**42**)

Carboxylate **7e** (16 mg, 0.05 mmol) afforded carboxamide **42** (22 mg, 77%) as a yellow oil: FT-IR (thin film, neat)  $\nu_{\text{max}}$  3424, 2960, 1674, 1528, 1500, 1265, 1214  $\text{cm}^{-1}$ ;  $^1\text{H}$  NMR (300 MHz,  $\text{CD}_3\text{OD}$ )  $\delta$  7.76 (d, 2H,  $J = 8.8$  Hz), 7.63 (d, 1H,  $J = 8.8$  Hz), 7.27–7.09 (m, 5H), 6.97 (d, 2H,  $J = 8.8$  Hz), 6.61 (d, 1H,  $J = 2.4$  Hz), 6.52 (dd, 1H,  $J = 2.6$ , 8.6 Hz), 4.14 (s, 3H), 4.06–4.00 (m, 4H), 3.04–2.09 (m, 6H), 2.05–2.00 (m, 2H), 1.80–1.73 (m, 2H), 1.54–1.46 (m, 2H), 1.20 (t, 6H,  $J = 7.2$  Hz), 0.95 (t, 3H,  $J = 7.3$  Hz);  $^{13}\text{C}$  NMR ( $\text{CDCl}_3$ , 125 MHz)  $\delta$  157.4, 157.2, 155.9, 149.2, 148.8, 143.6, 143.6, 137.3, 127.8, 127.0, 127.0, 125.0, 124.7, 121.9, 120.9, 120.5, 117.5, 117.5, 117.2, 104.8, 102.5, 99.8, 68.5, 66.1, 49.3, 46.9, 46.9, 39.4, 31.1, 25.8, 19.4, 13.9, 10.6, 10.6; LRMS (FAB)  $m/z$  589 ( $\text{M} + \text{H}^+$ ); HRMS (FAB) calcd for  $\text{C}_{34}\text{H}_{42}\text{FN}_4\text{O}_4$  ( $\text{M} + \text{H}^+$ ): 589.3190; found 589.3196; HPLC (5.27 min, 95.2%).

4.3.25. *N*-(2-butoxy-4-(3-(diethylamino)propoxy)phenyl)-3-(4-(3,4-difluorophenoxy)phenyl)-1-methyl-1H-pyrazole-5-carboxamide (**43**)

Carboxylate **13f** (16 mg, 0.05 mmol) afforded carboxamide **43** (11 mg, 40%) as a colorless oil:  $^1\text{H}$  NMR (300 MHz,  $\text{CD}_3\text{OD}$ )  $\delta$  7.81 (d, 2H,  $J = 8.6$  Hz), 7.63 (d, 1H,  $J = 8.8$  Hz), 7.26 (q, 1H,  $J = 9.7$  Hz), 7.15 (s, 1H), 7.05 (d, 2H,  $J = 8.3$  Hz), 6.99–6.93 (m, 1H), 6.83–6.80 (m, 1H), 6.65–6.56 (m, 2H), 4.16 (s, 3H), 4.11–4.03 (m, 4H), 3.38–3.18 (m, 6H), 2.21–2.19 (m, 2H), 1.80–1.79 (m, 2H), 1.52 (q, 2H,  $J = 7.5$  Hz), 1.33–1.28 (m, 6H), 0.96 (t, 3H,  $J = 7.4$  Hz);  $^{13}\text{C}$  NMR ( $\text{CDCl}_3$ , 75 MHz)  $\delta$  157.2, 156.7, 155.9, 155.6, 153.3, 149.0, 148.8, 137.3, 128.6, 127.2, 127.2, 121.0, 120.6, 119.2, 119.2, 117.7, 117.5, 114.4, 108.6, 104.9, 102.6, 99.9, 68.6, 66.1, 49.3, 46.8, 46.8, 39.4, 31.2, 29.7, 19.4, 13.9, 10.3, 10.3; LRMS (FAB)  $m/z$  607 ( $\text{M} + \text{H}^+$ ); HRMS (FAB) calcd for  $\text{C}_{34}\text{H}_{41}\text{F}_2\text{N}_4\text{O}_4$  ( $\text{M} + \text{H}^+$ ): 607.3090; found 607.3096; HPLC (6.10 min, 95.1%).

4.3.26. *N*-(2-butoxy-4-(3-(diethylamino)propoxy)phenyl)-3-(4-(3-chloro-4-methoxyphenoxy)phenyl)-1-methyl-1H-pyrazole-5-carboxamide (**44**)

Carboxylate **13h** (7 mg, 0.02 mmol) afforded carboxamide **44** (6 mg, 52%) as a colorless oil:  $^1\text{H}$  NMR (500 MHz,  $\text{CD}_3\text{OD}$ )  $\delta$  7.77 (d, 2H,  $J = 8.5$  Hz), 7.62 (d, 1H,  $J = 8.7$  Hz), 7.12 (s, 1H), 7.08–7.06 (m, 2H), 6.99–6.95 (m, 3H), 6.63 (d, 1H,  $J = 2.4$  Hz), 6.54 (dd, 1H,  $J = 2.2$ , 8.7 Hz), 4.16 (s, 3H), 4.08 (t, 2H,  $J = 5.8$  Hz), 4.03 (t, 2H,  $J = 7.5$  Hz), 3.87 (s, 3H), 3.09 (t, 2H,  $J = 7.9$  Hz), 3.01 (q, 4H,  $J = 4.8$  Hz), 2.12–2.07 (m, 2H), 1.82–1.76 (m, 2H), 1.55–1.48 (m, 2H), 1.24 (t, 6H,  $J = 7.3$  Hz), 0.96 (t, 3H,  $J = 7.4$  Hz);  $^{13}\text{C}$  NMR ( $\text{CDCl}_3$ , 125 MHz)  $\delta$  157.7, 155.9, 151.6, 150.3, 149.2, 148.8, 137.3, 127.8, 127.0, 127.0, 123.1, 121.7, 120.9, 120.5, 118.5, 118.3, 118.3, 112.8, 104.8, 102.5, 99.9, 68.5, 66.2, 56.6, 49.3, 46.9, 46.9, 39.4, 31.2, 29.7, 19.4, 13.9, 10.6, 10.6; LRMS (FAB)  $m/z$  635 ( $\text{M} + \text{H}^+$ ); HRMS (FAB) calcd for  $\text{C}_{35}\text{H}_{44}\text{ClN}_4\text{O}_5$  ( $\text{M} + \text{H}^+$ ): 635.3000; found 635.2995; HPLC (4.57 min, 98.7%).

4.3.27. *N*-(2-butoxy-4-(3-(diethylamino)propoxy)phenyl)-3-(4-(3-fluoro-4-methoxyphenoxy)phenyl)-1-methyl-1H-pyrazole-5-carboxamide (**45**)

Carboxylate **13g** (7 mg, 0.02 mmol) afforded carboxamide **45** (6 mg, 51%) as a colorless oil:  $^1\text{H}$  NMR (300 MHz,  $\text{CD}_3\text{OD}$ )  $\delta$  7.77 (d,

$^1\text{H}$ ,  $J = 8.8$  Hz), 7.62 (d,  $^1\text{H}$ ,  $J = 8.6$  Hz), 7.12–7.05 (m, 2H), 7.00 (d,  $^1\text{H}$ ,  $J = 8.8$  Hz), 6.87–6.77 (m, 2H), 6.63 (d,  $^1\text{H}$ ,  $J = 2.4$  Hz), 6.54 (dd,  $^1\text{H}$ ,  $J = 2.6$ , 8.8 Hz), 4.16 (s, 3H), 4.08–4.02 (m, 4H), 3.86 (s, 3H), 3.05–2.91 (m, 6H), 2.11–2.00 (m, 2H), 1.83–1.74 (m, 2H), 1.58–1.45 (m, 2H), 1.21 (t, 6H,  $J = 7.2$  Hz), 0.96 (t, 3H,  $J = 7.4$  Hz);  $^{13}\text{C}$  NMR ( $\text{CDCl}_3$ , 75 MHz)  $\delta$  157.5, 157.1, 156.0, 155.5, 154.3, 149.2, 148.8, 137.3, 127.8, 127.0, 127.0, 120.9, 120.4, 118.4, 118.4, 114.6, 110.0, 108.6, 108.3, 104.8, 102.5, 99.9, 68.5, 66.3, 56.8, 49.3, 46.9, 46.9, 39.4, 31.2, 26.1, 19.4, 13.9, 10.9, 10.9; LRMS (FAB)  $m/z$  619 ( $\text{M} + \text{H}^+$ ); HRMS (FAB) calcd for  $\text{C}_{35}\text{H}_{44}\text{FN}_4\text{O}_5$  ( $\text{M} + \text{H}^+$ ): 619.3296; found 619.3290; HPLC (3.96 min, 99.0%).

#### 4.4. Molecular modeling

##### 4.4.1. Preparation of molecular structures

All computational simulations were performed using the Sybyl–X 1.3 software package (Tripos, Inc., St. Louis, MO) [36] based on CentOS Linux 5.7. The structures of compounds were prepared in MOL2 format using the sketcher module. Gasteiger–Hückel charges were assigned to ligand atoms. The structure of molecule was energy optimized using the conjugate gradient method and terminated when the energy gradient convergence criterion reached  $0.001 \text{ kcal mol}^{-1} \text{ \AA}^{-1}$ . The conformer library for all compounds was stored in a database.

##### 4.4.2. Preparation of target protein structure and flexible docking

The X-ray structure of RAGE (PDB id: 3O3U) [33] was retrieved from the PDB (Protein Data Bank). All crystallographic water molecules were removed and all amino acid side chains were fixed. The active site was defined within  $3.0 \text{ \AA}$  radius of specific amino acid residues (LYS43, LYS44, ARG48, and ARG104) which play important roles as described in literatures [25,37]. The docking and subsequent scoring were performed using the default parameters of the Surflex-Dock program implanted in the Sybyl-X 1.3. Final scores for all Surflex-Dock solutions were calculated by a consensus scoring method (CScore) and used for database ranking. After visual inspection of docked poses, one of the conformers having high consensus score (CScore = 5 or 4) was selected for the best docking pose described in the text. Figures are made by using the program 3D Explorer [38].

#### 4.5. Biological study

##### 4.5.1. Preparation of biotinylated-human-RAGE and human $\text{A}\beta$ 1–42 [19]

Biotinylated-human-RAGE proteins and  $\text{A}\beta$  were prepared according to established protocols. The  $\text{A}\beta$  stock in DMSO was diluted directly into phosphate-buffered saline (PBS) prior to use, and  $10 \mu\text{M}$   $\text{A}\beta$  in a PBS solution was incubated for 24 h at  $4 \text{ }^\circ\text{C}$  to generate oligomeric aggregates.

##### 4.5.2. ELISA test

One microgram of purified biotinylated-human-RAGE,  $1 \mu\text{L}$  of  $10 \mu\text{M}$   $\text{A}\beta$  solution and  $20 \mu\text{M}$  of the compound in  $100 \mu\text{L}$  of TBS-T containing 2.5% BSA were incubated on a streptavidin-coated plate for 60 min at ambient temperature. After washing the plate with TBS-T, a horseradish-peroxidase conjugated 4G8 antibody (4G8-HRP, 1:1000 dilution) in  $100 \mu\text{L}$  of TBS-T containing 2.5% BSA was added into each well to detect the bound  $\text{A}\beta$ . The plate was incubated for 60 min at ambient temperature. After washing with TBS-T, the plate was developed using TMB substrate and the reaction was stopped with sulfuric acid. The absorbance was read on a Sunrise plate reader (TECHAN) at 450 nm.

##### 4.5.3. Acute model study

ICR mice were obtained from SAMTACO (Korea). A single dose of the test compound ( $25 \text{ mg/kg}$ ) or vehicle was administered by intraperitoneal (i.p.) injection to 3 month-old ICR mice ( $25 \text{ g}$ ,  $n = 4$ , male). After 20 min,  $200 \mu\text{L}$  of  $25 \mu\text{M}$  human  $\text{A}\beta$ 1–42 in PBS was injected into the tail vein and allowed to circulate for 30 min. Prior to the sacrifice of the mice used to determine the level of human  $\text{A}\beta$  in the brain, blood samples were drawn from the retro-orbital plexus using EDTA-coated capillary tubes to determine the level of circulating human  $\text{A}\beta$ .

#### Acknowledgments

This work was supported by National Research Foundation grant funded by the Korea government (MEST) as a part of Global Drug Candidate Development Program for Neurodegenerative Diseases (2011-0018334) and the National Research Foundation of Korea Grant funded by the Korean Government (MEST) (NRF-C1ABA001-2013-045137).

#### Appendix A. Supplementary data

Supplementary data related to this article can be found at <http://dx.doi.org/10.1016/j.ejmech.2014.03.072>.

#### References

- [1] D.J. Selkoe, Alzheimer's disease: genes, proteins, and therapy, *Physiological Reviews* 81 (2001) 741–766.
- [2] J. Hardy, D.J. Selkoe, The amyloid hypothesis of Alzheimer's disease: progress and problems on the road to therapeutics, *Science* 297 (2002) 353–356.
- [3] K. Blennow, M.J. de Leon, H. Zetterberg, Alzheimer's disease, *Lancet* 368 (2006) 387–403.
- [4] Y.J. Wang, H.D. Zhou, X.F. Zhou, Clearance of amyloid-beta in Alzheimer's disease: progress, problems and perspectives, *Drug Discovery Today* 11 (2006) 931–938.
- [5] R.E. Tanzi, R.D. Moir, S.L. Wagner, Clearance of Alzheimer's  $\text{A}\beta$  peptide: the many roads to perdition, *Neuron* 43 (2004) 605–608.
- [6] R. Deane, D.S. Yan, R.K. Subramanian, B. LaRue, S. Jovanovic, E. Hogg, D. Welch, L. Manness, C. Lin, J. Yu, H. Zhu, J. Ghiso, B. Frangione, A. Stern, A.M. Schmidt, D.L. Armstrong, B. Arnold, B. Liliensiek, P. Nawroth, F. Hofman, M. Kindy, D. Stern, B. Zlokovic, RAGE mediates amyloid-beta peptide transport across the blood-brain barrier and accumulation in brain, *Natural Medicines* 9 (2003) 907–913.
- [7] L. Lin, RAGE on the toll road? *Cellular & Molecular Immunology* 3 (2006) 351–358.
- [8] H. Huttunen, C. Fages, H. Rauvala, Receptor for advanced glycation end products (RAGE)-mediated neurite outgrowth and activation of NF- $\kappa$ B require the cytoplasmic domain of the receptor but different downstream signaling pathways, *Journal of Biological Chemistry* 274 (1999) 19919–19924.
- [9] J. Li, A.M. Schmidt, Characterization and functional analysis of the promoter of RAGE, the receptor for advanced glycation end products, *Journal of Biological Chemistry* 272 (1997) 16498–16506.
- [10] A. Bierhaus, S. Schiekofer, M. Schwaninger, M. Andrassy, P.M. Humpert, J. Chen, M. Hong, T. Luther, T. Henle, I. Klotting, M. Morcos, M. Hofmann, H. Tritschler, B. Weigle, M. Kasper, M. Smith, G. Perry, A.M. Schmidt, D.M. Stern, H.U. Haring, E. Schleicher, P.P. Nawroth, Diabetes-associated sustained activation of the transcription factor nuclear factor- $\kappa$ B, *Diabetes* 50 (2001) 2792–2808.
- [11] M. Sakono, T. Zako, Amyloid oligomers: formation and toxicity of  $\text{A}\beta$  oligomers, *FEBS Journal* 277 (2010) 1348–1358.
- [12] C. Holmes, D. Boche, D. Wilkinson, G. Yadegarfar, V. Hopkins, A. Bayer, R.W. Jones, R. Bullock, S. Love, J.W. Neal, E. Zotova, J.A. Nicoll, Long-term effects of  $\text{A}\beta$ 42 immunisation in Alzheimer's disease: follow-up of a randomised, placebo-controlled phase I trial, *Lancet* 372 (2008) 216–223.
- [13] O.G. Aderinwale, H.W. Ernst, S.A. Mousa, Current therapies and new strategies for the management of Alzheimer's disease, *American Journal of Alzheimer's Disease and Other Dementias* 25 (2010) 414–424.
- [14] L. Zhang, R. Postina, Y. Wang, Ectodomain shedding of the receptor for advanced glycation end products: a novel therapeutic target for Alzheimer's disease, *Cellular and Molecular Life Sciences* 66 (2009) 3923–3935.
- [15] D. Geroldi, C. Falcone, E. Emanuele, Soluble receptor for advanced glycation end products: from disease marker to potential therapeutic target, *Current Medicinal Chemistry* 13 (2006) 1971–1978.
- [16] M.N. Sabbagh, A. Agro, J. Bell, P.S. Aisen, E. Schweizer, D. Galasko, PF-04494700, an oral inhibitor of receptor for advanced glycation end products

- (RAGE), in Alzheimer disease, *Alzheimer Disease and Associated Disorders* 25 (2011) 206–212.
- [17] V. Srikanth, A. Maczurek, T. Phan, M. Steele, B. Westcott, D. Juskiw, G. Münch, Advanced glycation endproducts and their receptor RAGE in Alzheimer's disease, *Neurobiology of Aging* 32 (2011) 763–777.
- [18] R. Deane, I. Singh, A.P. Sagare, R.D. Bell, N.T. Ross, B. Larue, R. Love, S. Perry, N. Paquette, R.J. Deane, T. Meenakshisundaram, T. Zarcone, G. Fritz, A.E. Friedman, B.L. Miller, B.V. Zlokovic, A multimodal RAGE-specific inhibitor reduces amyloid  $\beta$ -mediated brain disorder in a mouse model of Alzheimer disease, *The Journal of Clinical Investigation* 122 (2012) 1377–1392.
- [19] Y.T. Han, G.-I. Choi, D. Son, N.-J. Kim, H. Yun, S. Lee, D.-J. Chang, H.-S. Hong, H. Kim, H.-J. Ha, Y.-H. Kim, H.-J. Park, J. Lee, Y.-G. Suh, Ligand-based design, synthesis and biological evaluation of 2-aminopyrimidines, a novel series of RAGE (receptor for advanced glycation end products) inhibitors, *Journal of Medicinal Chemistry* 55 (2012) 9120–9135.
- [20] For synthetic methods of pyrazole-5-carboxamides, see: (a) I. Vujanovic, A. Paravic-Radicevic, K. Mlinaric-Majerski, K. Brajsa, B. Bertosa, Synthesis and biological validation of novel pyrazole derivatives with anticancer activity guided by 3D-QSAR analysis, *Bioorganic & Medicinal Chemistry* 20 (2012) 2101–2110; (b) B.F. Bonini, M.C. Franchini, D. Gentili, E. Locatelli, A. Ricci, 1,3-Dipolar cycloaddition of nitrile imines with functionalised acetylenes. Regiocontrolled Sc(OTf)<sub>3</sub> catalyzed synthesis of 4- and 5-substituted pyrazoles, *Synlett* 14 (2009) 2328–2332; (c) H. Zou, H. Zhu, J. Shao, J. Wu, W. Chen, M.A. Giulianotti, Y. Yu, A facile approach to polysubstituted pyrazoles from hydrazonyl chlorides and vinyl azides, *Tetrahedron* 67 (2011) 4887–4891.
- [21] W.H. Heath, F. Palmieri, J.R. Adams, B.K. Long, J. Chute, T.W. Holcombe, S. Zieren, M.J. Truitt, J.L. White, C.G. Willson, Degradable cross-linkers and strippable imaging materials for step-and-flash imprint lithography, *Macromolecules* 41 (2008) 719–726.
- [22] N.E. Faucher, P. Martres, Substituted pyrazoles as PPAR agonists, WO2005/049578(A1).
- [23] D.A. Evans, J.L. Katz, T.R. West, Synthesis of diary ethers through the copper-promoted arylation of phenols with arylboronic acids. An expedient synthesis of thyroxine, *Tetrahedron Letters* 39 (1998) 2937–2940.
- [24] V. Bertolasi, P. Gilli, V. Ferretti, G. Gilli, C. Fernández-Castaño, Self-assembly of NH-pyrazoles via intermolecular N-H...N hydrogen bonds, *Acta Crystallographica B55* (1999) 985–993.
- [25] S. Matsumoto, T. Yoshida, H. Murata, S. Harada, N. Fujita, S. Nakamura, Y. Yamamoto, T. Watanabe, H. Yonekura, H. Yamamoto, T. Ohkubo, Y. Kobayashi, Solution structure of the variable-type domain of the receptor for advanced glycation end products: new insight into AGE-RAGE interaction, *Biochemistry* 47 (47) (2008) 12299–12311.
- [26] N. Zacharias, D.A. Dougherty, Cation- $\pi$  interactions in ligand recognition and catalysis, *TRENDS in Pharmacological Sciences* 23 (2002) 281–287.
- [27] L.H. Takahashi, R. Radhakrishnan, R.E. Rosenfield, E.F. Meyer, D.A. Trainor, Crystal structure of the covalent complex formed by a peptidyl  $\alpha,\alpha$ -difluoro- $\beta$ -keto amide with porcine pancreatic elastase at 1.78 Å resolution, *Journal of the American Chemical Society* 111 (1989) 3368–3374.
- [28] E. Istvan, J. Deisenhofer, Structural mechanism for statin inhibition of HMG-CoA reductase, *Science* 292 (2001) 1160–1164.
- [29] G. Sidhu, S.G. Withers, N.T. Nguyen, L.P. McIntosh, L. Ziser, G.D. Brayer, Sugar ring distortion in the glycosyl-enzyme intermediate of a family G/11 xylanase, *Biochemistry* 38 (1999) 5346–5354.
- [30] P. Gonin, Y. Xu, L. Milon, S. Dabernat, M. Morr, R. Kumar, M.L. Lacombe, J. Janin, I. Lascu, Catalytic mechanism of nucleoside diphosphate kinase investigated using nucleotide analogues, viscosity effects, and X-ray crystallography, *Biochemistry* 38 (1999) 7256–7272.
- [31] H.J. Böhm, D. Banner, S. Bendels, M. Kansy, B. Kuhn, K. Müller, U. Obst-Sander, M. Stahl, Fluorine in medicinal chemistry, *ChemBioChem* 5 (2004) 637–643.
- [32] M.T. Scerba, C.M. Leavitt, M.E. Diener, A.F. DeBlase, T.L. Guasco, M.A. Siegler, N. Bair, M.A. Johnson, T. Lectka, NH<sup>+</sup>-F hydrogen bonding in a fluorinated "proton sponge" derivative: Integration of solution, solid-state, gas-phase, and computational studies, *Journal of Organic Chemistry* 76 (2011) 7975–7984.
- [33] H. Park, J.C. Boyington, The 1.5 Å crystal structure of human receptor for advanced glycation endproducts (RAGE) ectodomains reveals unique features determining ligand binding, *Journal of Biological Chemistry* 285 (2010) 40762–40770.
- [34] The details of pharmacokinetic investigation on 40 will be reported soon.
- [35] C.D. Bevan, R.S. Lloyd, A high-throughput screening method for the determination of aqueous drug solubility using laser nephelometry in microtiter plates, *Analytical Chemistry* 72 (2000) 1781–1787.
- [36] Sybyl-X, 1.3 (Ed.); SYBYL Molecular Modeling Software, Tripos Inc.: St. Louis, MO, 2011.10.
- [37] D. Stern, S.D. Yan, A.M. Schmidt, I. Lamster, Ligand binding site of rage and uses thereof, US 6555651B2, 2003.
- [38] Benchware® 3D Explorer; 3D Chemical Visualization and Decision Support, Tripos Inc.: St. Louis, MO, 2011.10.